errata

Protein memory through altered folding mediated by intramolecular chaperones

U. P. Shinde, J. J. Liu & M. Inouye

Nature **389,** 520–522 (1997)

Three of the superscripts in Fig. 3b of this Letter were incorrect. The amended figure is shown below. □

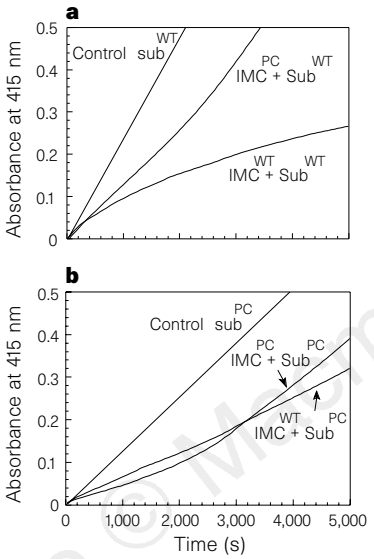

G-protein-coupled receptor of Kaposi's sarcoma-associated herpesvirus is a viral oncogene and angiogenesis activator

Carlos Bais, Bianca Santomasso, Omar Coso, Leandros Arvanitakis, Elizabeth Geras Raaka, J. Silvio Gutkind, Adam S. Asch, Ethel Cesarman, Marvin C. Gershengorn & Enrique A. Mesri

Nature **391,** 86–89 (1998)

The name of the penultimate author of this Letter was misspelled: his name is Marvin C. Gershengorn. □

correction

A GPI-linked protein that interacts with Ret to form a candidate neurturin receptor

Robert D. Klein, Daniel Sherman, Wei-Hsien Ho, Donna Stone, Gregory L. Bennett, Barbara Moffat, Richard Vandlen, Laura Simmons, Qimin Gu, Jo-Anne Hongo, Brigitte Devaux, Kris Poulsen, Mark Armanini, Chika Nozaki, Naoya Asai, Audrey Goddard, Heidi Phillips, Chris E. Henderson, Masahide Takahashi & Arnon Rosenthal

Nature **387,** 717–721 (1997)

An error in the designation of address symbols has caused confusion over the following authors' affiliations: R.D.K.'s present address is at Deltagen Inc.; L.S. Q.G. and A.G. are at Genentech Inc. □

KNOW YOUR COPY RIGHTS
RESPECT OURS

The publication you are reading is protected by copyright law.

Photocopying copyright material without permission is no different from stealing a magazine from a newsagent, only it doesn't seem like theft.

If you take photocopies from books, magazines and periodicals at work your employer should be licensed with CLA.

Make sure you are protected by a photocopying licence.

CLA

The Copyright Licensing Agency Limited
90 Tottenham Court Road, London W1P 0LP
Telephone: 0171 436 5931 Fax: 0171 436 3986

Nature © Macmillan Publishers Ltd 1998

Nature © Macmillan Publishers Ltd 1998

Protein memory through altered folding mediated by intramolecular chaperones

U. P. Shinde, J. J. Liu & M. Inouye

Department of Biochemistry, Robert Wood Johnson Medical School-UMDNJ, 675 Hoes Lane, Piscataway, New Jersey 08854, USA

The 77-residue propeptide of subtilisin acts as an intramolecular chaperone that organizes the correct folding of its own protease domain. Similar folding mechanisms are used by several prokaryotic and eukaryotic proteins, including prohormone-convertases. Here we show that the intramolecular chaperone of subtilisin facilitates folding by acting as a template for its protease domain, although it does not form part of that domain. Subtilisin E folded by an intramolecular chaperone with an Ile(−48)-to-Val mutation acquires an 'altered' enzymatically active conformation that differs from wild-type subtilisin E. Although both the altered and wild-type subtilisins have identical amino-acid sequences, as determined by amino-terminal sequencing and mass spectrometry, they bind their cognate intramolecular chaperones with 4.5-fold greater affinity than non-cognate intramolecular chaperones, when added *in trans*. The two subtilisins also have different secondary structures, thermostability and substrate specificities. Our results indicate that an identical polypeptide can fold into an altered conformation through a mutated intramolecular chaperone and maintains memory of the folding process. Such a phenomenon, which we term 'protein memory', may be important in investigations of protein folding.

The amino-acid sequence encodes all the information necessary for a protein to adopt its three-dimensional structure[1]. Protein folding describes the transition of a non-functional polypeptide into a functional protein molecule[2]. Some proteins require an intramolecular chaperone (IMC) to act as a single turn-over catalyst to mediate correct folding[3–7]. Upon folding, the IMC is removed through an autolytic[3] or exogenous proteolytic activity. Subtilisin[3,7–10], α-lytic protease[11], aqualysin[12] and carboxypeptidase Y[13] constitute some well-studied examples of such proteins. Subtilisin undergoes conformational changes upon autoprocessing of its IMC domain[14]. At low concentrations and in the absence of their IMC domains, subtilisin and α-lytic protease acquire molten-globule-like intermediate states[15–17]. Addition of IMC domains *in trans* promotes these intermediates to surmount the activation energy barrier between the intermediate and the native states[15,17], suggesting that IMCs help overcome kinetic barriers during the late stages of folding[15,16,18]. They also function as temporary inhibitors of enzymatic activity[19,20].

The *in vitro* maturation pathway of pro-subtilisin E involves folding, autoprocessing and degradation of its 77-residue IMC domain, resulting in a 275-residue protease domain. An I–48V mutation within the IMC has been isolated[21]. Mutant and wild-type pro-subtilisins and IMC domains were cloned, expressed and purified in *Escherichia coli* using vectors pHI215T (ref. 21) and pET11a (ref. 22). Proteins were refolded and then analysed using SDS–PAGE (polyacrylamide gel electrophoresis). Wild-type and mutant precursors autoprocess and degrade their IMC domains to generate the enzymatically active proteins wild-type subtilisin (Sub^{WT}) and the 'altered' subtilisin (Sub^{PC}) (Fig. 1a). Both Sub^{WT} and Sub^{PC} display similar retention times on an analytical gel-filtration column (Fig. 1b), suggesting their corresponding Stokes radii are similar. Moreover, the proteins do not contain partly or completely unfolded polypeptides. Mass spectroscopy shows that the relative molecular mass (M_r) of both Sub^{PC} (27,719 ± 10) and Sub^{WT} (27,728 ± 10) are within range of the theoretical M_r of subtilisin E (27,720), expressed using the vector pHI215T (ref. 21). Amino-terminal sequencing shows that both proteins have identical amino termini. Circular dichroism spectra (Fig. 1c) indicate that Sub^{WT} and Sub^{PC} display similar but not identical secondary structures and represent homogenous but structurally distinct folded protein populations.

The catalytic properties of Sub^{WT} and Sub^{PC} were estimated using *N*-succinyl-AAPF-*p*-nitroanilide as a substrate[3,24]. Sub^{WT} and Sub^{PC}

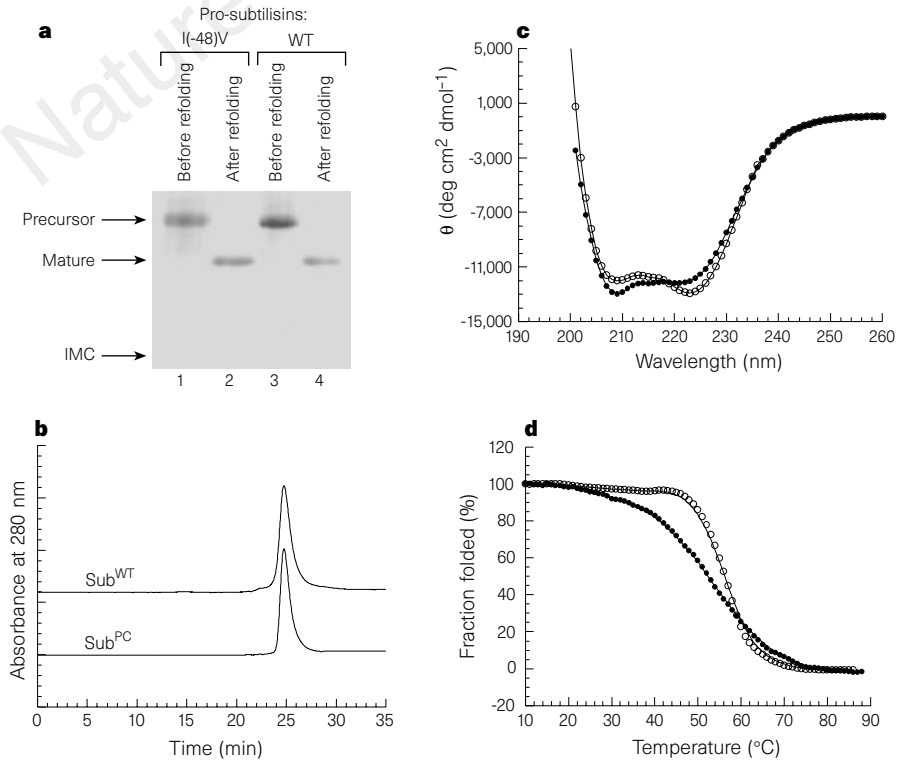

Figure 1 a, Maturation of wild-type (WT) and Ile(–48)Val mutant pro-subtilisin. The refolded proteins were electrophoresed on a 17.5% acrylamide gel. Lanes 1 and 2 represent the Ile(–48)Val mutant, and lanes 3 and 4 represent wild-type pro-subtilisins before and after refolding. **b**, Analytical gel-filtration chromatography of Sub^{WT} and Sub^{PC} after refolding. Sub^{PC} (lane 2 in **a**) and Sub^{WT} (lane 4 in **a**) were applied on a TSK2000 column and eluted using 10 mM phosphate buffer, pH 7.0, containing 0.5 M ammonium sulphate, 1 mM $CaCl_2$, with a flow rate of 0.5 ml min^{-1}. **c**, Circular-dichroism spectra of Sub^{WT} (open circles) and Sub^{PC} (filled circles). Temperature was maintained at 25 °C. **d**, Thermal unfolding of Sub^{WT} and Sub^{PC}. The fraction unfolded was monitored using circular dichroism and recording the changes in negative ellipiticity at 222 nm as a function of temperature. Unfolding of Sub^{PC} (filled circles) is less cooperative than Sub^{WT} (open circles).

Nature © Macmillan Publishers Ltd 1997

Table 1 Properties of Sub^{WT} and Sub^{PC}

Property	Sub^{WT}	Sub^{PC}
K_M for succinyl-AAPF-*p*-nitroanilide ($\times 10^{-3}$ M)	2.040 ± 0.015	0.675 ± 0.005
K_{cat} for succinyl-AAPF-*p*-nitroanilide (s^{-1})	22.000 ± 0.15	11.800 ± 0.080
K_{cat}/K_M ($s^{-1} \times 10^3$ M)	10.8	17.5
Apparent K_i for IMC^{WT} ($\times 10^{-9}$ M)	153	694
Apparent K_i for IMC^{PC} ($\times 10^{-9}$ M)	846*	184*
Activity for succinyl-AAPF-*p*-nitroanilide (%)	100	54
Activity for succinyl-AAA-*p*-nitroanilide (%)	100	71
Activity for succinyl-AAL-*p*-nitroanilide (%)	100	88

* Calculated from data for 600 s because after this time rapid degradation of the IMC occurs.

display a K_M of 2.040 ± 0.015 and 0.675 ± 0.005 mM, respectively (Table 1). The K_{cat}/K_M ratio for Sub^{PC} is 62% greater than that for Sub^{WT}. Interactions between subtilisin and the IMC follow slow-binding inhibition kinetics[22,24,25]. Estimated values of the inhibition constant K_i of IMC^{WT} and IMC^{PC} for Sub^{WT} and Sub^{PC} show that IMC^{PC} binds Sub^{WT} with an apparent K_i that is 4.6-fold higher than its apparent K_i for Sub^{PC}, whereas IMC^{WT} binds Sub^{PC} 4.5-fold weaker than with Sub^{WT} (Table 1). If Sub^{WT} and Sub^{PC} are denatured and refolded using IMC^{WT} *in trans*, both display similar kinetics towards *N*-succinyl-AAPF-*p*-nitroanilide. Incubating folded Sub^{PC} with IMC^{WT} did not change the catalytic properties of Sub^{PC} to Sub^{WT}.

The thermostabilities of Sub^{WT} and Sub^{PC} were determined by monitoring changes in negative ellipiticity at 222 nm (Fig. 1d). Sub^{PC} was found to be relatively unstable (melting temperature, T_m, 52 °C) and less cooperative than Sub^{WT} (T_m, 58.5 °C). The X-ray structure of the IMC^{WT}-subtilisin complex[23] leads us to speculate on domains that may be affected. There are important interactions between the IMC domain and subtilisin between residues 100 and 144. Ile(−48) in the IMC is buried inside a hydrophobic core constituted by four β-sheets and two α-helices. The I–48V substitution may create a cavity within the hydrophobic core which perturbs the final structure of the protease domain. Structural changes resulting from mutations of surface residues in lysozyme are localized near the mutation, whereas those involving buried residues may be transmitted to other parts of the protein[26]. Similar structural alterations may affect surface charge distribution in subtilisin, which can alter its enzymatic properties[27]. The relative activities of Sub^{WT} and Sub^{PC} towards *N*-succinyl-AAPF-*p*-nitroanilide, *N*-succinyl-AAA-*p*-nitroanilide and *N*-succinyl-AAL-*p*-nitroanilide are different (Table 1).

Protease domains degrade IMCs upon completing protein folding[22]. To further characterize Sub^{WT} and Sub^{PC}, we analysed their interactions with IMC^{WT} and IMC^{PC}. IMC^{WT} acquires significant secondary structure only after interacting with subtilisin[7,15,23], and slow-binding inhibition kinetics may represent the time required for the IMC to fold/bind the protease domain. Inhibition kinetics were analysed using two different approaches. First, concentrations of Sub^{WT} and Sub^{PC} were adjusted such that their velocities for cleaving *N*-AAPF-*p*-nitroanilide were identical. Suitable enzyme concentrations were selected[22,25] and reactions were initiated by addition of Sub^{WT} or Sub^{PC}. IMC^{WT} inhibited Sub^{WT} more than Sub^{PC} (Fig. 2a), whereas IMC^{PC} initially inhibited Sub^{PC} more than Sub^{WT} but was subsequently degraded rapidly to release inhibition (Fig. 2b). A similar phenomenon can be observed with IMC^{WT}, but not in the timescale of these experiments. In the second approach, concentrations of Sub^{WT} and Sub^{PC} were identical and reactions were performed as before. IMC^{PC} bound weakly to Sub^{WT} when compared with IMC^{WT} (Fig. 3a), whereas IMC^{PC} bound Sub^{PC} initially with greater affinity, but was degraded more rapidly than IMC^{WT} (Fig. 3b).

These results indicate that IMCs imprint unique structural information onto their protease domain. Such structural imprinting, or 'protein memory', may be important for studies of protein folding. Our results also suggest that multiple, structurally distinct native structures can be encoded by unique amino-acid sequences. Although our studies were limited to subtilisin, this phenomenon addresses a general property of protein-folding mechanisms, as propeptides may not differ functionally from internal uncleaved sequences in proteins.

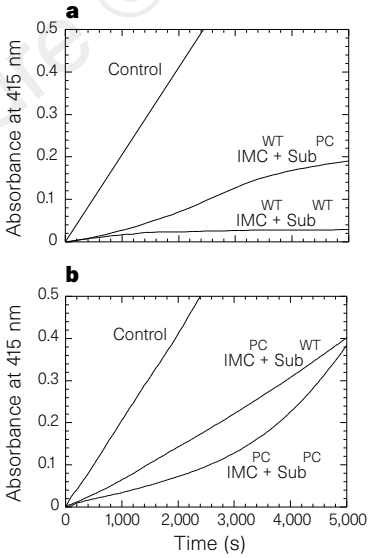

Figure 2 Comparison of inhibition profiles of Sub^{WT} and Sub^{PC}. Concentrations of the enzymes were maintained such that both Sub^{WT} and Sub^{PC} display the same units of activity towards the synthetic substrate *N*-succinyl-AAPF-*p*-nitroanilide. Reactions were performed at 23 °C, and substrate concentration maintained at 3 mM. Control depicts profiles of Sub^{WT} and Sub^{PC}, but only one has been shown because the two lines overlap. **a**, Inhibition profiles with IMC^{WT} (8.0 μM); **b**, inhibition profiles for IMC^{PC} (3.74 μM). IMC^{WT} interacts and binds tightly with Sub^{WT}, whereas IMC^{PC} binds tightly with Sub^{PC}.

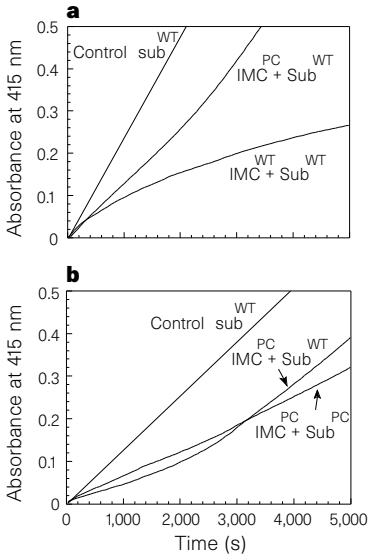

Figure 3 Comparison of inhibition profiles of Sub^{WT} and Sub^{PC}. The concentrations of Sub^{WT} and Sub^{PC} are identical (1.5 nM) but their units of enzymatic activity are different. Substrate and IMC concentrations were 3 mM and 1.0 μM, respectively. **a**, Inhibition of Sub^{WT} by IMC^{WT} and IMC^{PC}; **b** inhibition of Sub^{PC} by IMC^{WT} and IMC^{PC}. After 3,000 s, activity for the mixture of IMC^{PC} and Sub^{PC} is greater than that of IMC^{WT} and Sub^{PC}. This suggests that IMC^{PC} initially interacts and binds tightly to Sub^{PC} but is then rapidly degraded.

Nature © Macmillan Publishers Ltd 1997

Nature © Macmillan Publishers Ltd 1997

A phenomenon called enzyme memory was previously observed when subtilisin was lyophilized from aqueous solutions containing competitive inhibitors[28]. Subtilisin then became much more active in anhydrous solvents than subtilisin lyophilized in the absence of the inhibitors. However, enzyme memory differs from protein memory in that enzyme memory disappears in aqueous solutions owing to the conformational flexibility of enzymes[29], whereas IMC-imprinted protein memory seems to be stable in aqueous environments. Another important implication of our finding relates to the maturation of eukaryotic hormones mediated by a family of subtilisin-like prohormone-convertases[30]. Propeptides of some of these proteases function as IMCs, and it is possible that point mutations within the IMC domains may result in altered folding, and subsequent changes in substrate specificity of the enzyme may lead to hormonal disorders. □

Methods

Folding of subtilisin precursors. Refolding of precursors (50 μg ml^{-1}) was initiated through a dialysis procedure that involved stepwise removal of urea[14,16,22]. Dialysis was continued for 48 h after complete removal of urea. The refolded proteins were incubated at 37 °C for 6 h to facilitate propeptide degradation. This incubation can also be performed at 4 °C for an additional 48 h without affecting the kinetic data of the proteins. The proteins were concentrated using an ultrafiltration membrane with a cutoff at an M_r of 10K, and were dialysed at 4 °C for 24 h (using a tubing with a 12K cutoff) against refolding buffer (without urea) to remove contaminating peptide fragments that may have been generated by proteolysis[22]. They were subsequently purified using ion-exchange chromatography.

Slow-binding kinetics. The IMC domain of subtilisin behaves like a slow-binding inhibitor[22]. Experiments were therefore performed under pseudo-first-order kinetics, where the lowest IMC concentrations were greater than a 10-fold excess. Enzyme concentrations were set at levels low enough to give measurable rates of substrate hydrolysis, with observable state of inhibitor binding over the steady-state timescale. The IMC concentrations vary between 1 and 10 μM. Initial substrate concentration was 3 mM, and less than 10% of the substrate was degraded throughout the experiment. Reactions were initiated by addition of Sub^{WT} or Sub^{PC}. After thorough mixing, substrate cleavage was monitored by recording at 415 nm the release of *p*-nitroaniline. Data from each curve were fitted to the equation $A_{415} = \nu_s t + (\nu_o - \nu_s)(1 - e^{-k't})/k' + A_o$, where A_{415} is the absorbance at 415 nm, A_o is the initial absorbance, ν_o and ν_s are initial and final velocities, respectively, k' is the apparent first-order rate constant, and t is time. Curve fitting gives four independent variables (ν_o, ν_s, k' and A_o) at each inhibitor concentration. A plot of $(\nu_o - \nu_s)/\nu_s$ with different inhibitor concentrations $[I]$ was used to determine K_i.

Circular dichroism. Circular-dichroism measurements were performed on an automated Aviv-60DS spectrophotometer controlled by an online temperature-controlled unit. Purified protein (100 μg ml^{-1}) in 10 mM phosphate buffer, pH 7.0, containing 0.5 M $(NH_4)_2SO_4$, 1 mM $CaCl_2$ was filtered through 0.22-μm filter and scans were carried out between wavelengths of 260 and 190 nm in a cuvette with a 1-mm path length maintained at 25 °C. In the thermal unfolding experiments, temperatures were increased from 10 to 90 °C in 1 °C intervals, with a 30-s equilibration at each temperature. Data were collected at each temperature for 10 s. Protein solutions contain 1 mM PMSF to prevent autolysis during this procedure.

Received 21 February; accepted 3 July 1997.

1. Anfinsen, C. R. Principles that govern the folding of protein chains. *Science* **181,** 223–230 (1973).
2. Kim, P. S. & Baldwin, R. L. Intermediates in the folding reactions of small proteins. *Annu. Rev. Biochem.* **59,** 631–660 (1990).
3. Ikemura, H., Takagi, H. & Inouye, M. Requirement of pro-sequence for the production of active subtilisin E in *Escherichia coli*. *J. Biol. Chem.* **262,** 7859–7864 (1988).
4. Ikemura, H. & Inouye, M. *In vitro* processing of pro-subtilisin produced in *Escherichia coli*. *J. Biol. Chem.* **263,** 12959–12963 (1988).
5. Winther, J. R. & Sorensen, P. Propeptide of carboxypeptidase Y provides a chaperone-like function as well as inhibition of the enzymatic activity. *Proc. Natl Acad. Sci. USA* **88,** 9330–9334 (1991).
6. Richo, G. R. & Conner, G. E. Structural requirements of procathepsin D activation and maturation. *J. Biol. Chem.* **269,** 14806–14812 (1994).
7. Shinde, U., Li, Y., Chatterjee, S. & Inouye, M. Folding pathway mediated by an intramolecular chaperone. *Proc. Natl Acad. Sci. USA* **90,** 6924–6928 (1993).
8. Zhu, X., Ohta, Y., Jordan, F. & Inouye, M. Pro-sequence of subtilisin can guide the folding of denatured subtilisin in an intermolecular process. *Nature* **339,** 483–484 (1989).
9. Eder, J., Rheinnecker, M. & Fersht, A. Folding of subtilisin BPN′: role of the pro-sequence. *J. Mol. Biol.* **233,** 293–304 (1993).
10. Strausberg, S., Alexander, P., Wang, L., Schwarz, F. & Bryan, P. Catalysis of a protein folding reaction: thermodynamic and kinetic analysis of subtilisin BPN′ interactions with its propeptide fragment. *Biochemistry* **32,** 8112–8119 (1993).
11. Silen, J. L. & Agard, D. A. The α-lytic protease pro-region does not require a physical linkage to activate the protease domain *in vivo*. *Nature* **341,** 362–264 (1989).
12. Lee, Y. C., Ohta, T. & Matsuzawa, H. A non-covalent NH_2-terminal pro-region aids the production of active aqualysin I (a thermophilic protease) without the COOH-terminal pro-sequence in *Escherichia coli*. *FEMS Microbiol. Lett.* **92,** 73–78 (1992).
13. Winther, J. R., Sorensen, P. & Kielland-Brandt, M. C. Refolding of a carboxypeptidase Y folding intermediate *in vitro* by low-affinity binding of the proregion. *J. Biol. Chem.* **269,** 7006–7012 (1994).
14. Shinde, U. P. & Inouye, M. Folding mediated by an intramolecular chaperone: autoprocessing pathway of the precursor resolved via a 'substrate assisted catalysis' mechanism. *J. Mol. Biol.* **247,** 390–395 (1995).
15. Eder, J., Rheinnecker, M. & Fersht, A. Folding of subtilisin BPN′: characterization of a folding intermediate. *Biochemistry* **32,** 18–26 (1993).
16. Shinde, U. P. & Inouye, M. Folding pathway mediated by an intramolecular chaperone: characterization of the structural changes in pro-subtilisin E coincident with autoprocessing. *J. Mol. Biol.* **252,** 25–30 (1995).
17. Baker, D., Sohl, J. L. & Agard, D. A. A protein-folding reaction under kinetic control. *Nature* **356,** 263–265 (1992).
18. Eder, J. & Fersht, A. R. Pro-sequence assisted protein folding. *Mol. Microbiol.* **16,** 609–614 (1995).
19. Shinde, U. P. & Inouye, M. Intramolecular chaperones and protein folding. *Trends Biochem. Sci.* **18,** 442–446 (1993).
20. Bryan, P. in *Intramolecular Chaperones and Protein Folding* (eds Shinde, U. & Inouye, M.) 85–98 (R. G. Landes, Austin, TX, 1995).
21. Kobayashi, T. & Inouye, M. Functional analysis of the intramolecular chaperone. Mutational hot spots in the subtilisin pro-peptide and a second-site suppressor mutation within the subtilisin molecule. *J. Mol. Biol.* **226,** 931–933 (1992).
22. Li, Y., Hu, Z., Jordan, F. & Inouye, M. Functional analysis of the propeptide of subtilisin E as an intramolecular chaperone for protein folding, purification and characterization of mutant propeptides. *J. Biol. Chem.* **270,** 25127–25132 (1995).
23. Bryan, P. *et al.* Catalysis of a protein folding reaction: mechanistic implications of the 2.0 A structure of the subtilisin-prodomain complex. *Biochemistry* **34,** 10310–10318 (1995).
24. Jackson, S. E. & Fersht, A. R. Contribution of residues in the reactive site loop of chymotrypsin inhibitor 2 to protein stability and activity. *Biochemistry* **32,** 13909–13916 (1993).
25. Longstaff, C., Campbell, A. & Fersht, A. R. Recombinant chymotrypsin inhibitor 2: expression, kinetics analysis of inhibition fiwht a-chymotrypsin and wild-type and mutant subtilisin BPN′ and protein engineering to investigate inhibitory specificity and mechanism. *Biochemistry* **29,** 7339–7347 (1990).
26. Mathews, B. W. Studies on protein stability with T4 lysozyme. *Adv. Protein Chem.* **462,** 240–311 (1995).
27. Russel, A. J. & Fersht, A. R. Rational modification of enzyme catalysis by engineering surface charge. *Nature* **328,** 496–500 (1987).
28. Russell, A. J. & Klibanov, A. M. Inhibitor induced enzyme activation in organic solvents. *J. Biol. Chem.* **262,** 11624–11626 (1988).
29. Klibanov, A. M. What is remembered and why? *Nature* **374,** 596 (1995).
30. Barr, P. Mammalian subtilisins: the long-sought dibasic processing endoproteases. *Cell* **66,** 1–3 (1991).

Acknowledgements. We thank B. Chait and U. Mirza for mass spectroscopy, and K. Madura, K. Chada, H. Berman and B. Brodsky for discussions and for reading this manuscript.

Correspondence and requests for materials should be addressed to M.I. (e-mail: inouye@rwja.umdnj.edu).

Two-dimensional structure of plant photosystem II at 8-Å resolution

Kyong-Hi Rhee*†, Ed P. Morris‡, Daniela Zheleva‡, Ben Hankamer‡, Werner Kühlbrandt*† & James Barber‡

* *European Molecular Biology Laboratory, Meyerhofstrasse 1, D-69117 Heidelberg, Germany*

‡ *Wolfson Laboratories, Department of Biochemistry, Imperial College of Science, Technology and Medicine, London SW7 2AY, UK*

The photosystem II complex, which is the most abundant membrane protein in chloroplasts, comprises the light-harvesting complex II and a reaction-centre core. The reaction centre uses the solar energy collected by the light-harvesting complex II to withdraw electrons from water, releasing oxygen into the atmosphere. It thus generates an electrochemical potential, providing the energy for carbon dioxide fixation and the synthesis of organic molecules, which make up the bulk of the biosphere[1]. The structure of the light-harvesting complex II has been determined

† Present address: Max-Planck-Institut für Biophysik, Heinrich-Hoffmann-Strasse 7, D-60528, Frankfurt, Germany.

Nature © Macmillan Publishers Ltd 1997

proliferator-activated receptor gamma (PPAR gamma). *J. Biol. Chem.* **270,** 12953–12956 (1995).
8. Kliewer, S. A. *et al.* A prostaglandin J2 metabolite binds peroxisome proliferator-activated receptor gamma and promotes adipocyte differentiation. *Cell* **83,** 813–819 (1995).
9. Forman, B. M. *et al.* 15-Deoxy-delta 12,14-porostaglandin J2 is a ligand for the adipocyte determination factor PPAR gamma. *Cell* **83,** 803–812 (1995).
10. Lehmann, J. M., Lenhard, J. M., Oliver, B. B., Ringold, G. M. & Kliewer, S. A. Peroxisome proliferator-activated receptors alpha and gamma are activated by indomethacin and other non-steroidal anti-inflammatory drugs. *J. Biol. Chem.* **272,** 3406–3410 (1997).
11. Hotamisligil, G. S., Shargill, N. S. & Spiegelman, B. M. Adipose expression of tumor necrosis factor-alpha: direct role in obesity-linked insulin resistance. *Science* **259,** 87–91 (1993).
12. Patton, J. S. *et al.* Interferons and tumor necrosis factors have similar catabolic effects on 3T3 L1 cells. *Proc. Natl Acad. Sci. USA* **83,** 8313–8317 (1986).
13. Torti, F. M., Torti, S. V., Larrick, J. W. & Ringold, G. M. Modulation of adipocyte differentiation by tumor necrosis factor and transforming growth factor beta. *J. Cell Biol.* **108,** 1105–1113 (1989).
14. Marshall, M. K., Doerrler, W., Feingold, K. R. & Grunfeld, C. Leukemia inhibitory factor induces changes in lipid metabolism in cultured adipocytes. *Endocrinology* **135,** 141–147 (1994).
15. Berg, M., Fraker, D. L. & Alexander, H. R. Characterization of differentiation factor/leukaemia inhibitory factor effect on lipoprotein lipase activity and mRNA in 3T3-L1 adipocytes. *Cytokine* **6,** 425–432 (1994).
16. Lang, C. H., Dobrescu, C. & Bagby, G. J. Tumor necrosis factor impairs insulin action on peripheral glucose disposal and hepatic gluose output. *Endocrinology* **130,** 43–52 (1992).
17. Szalkowski, D., White-Carrington, S., Berger, J. & Zhang, B. Antidiabetic thiazolidinediones block the inhibitory effect of tumor necrosis factor-alpha on differentiation, insulin-stimulated glucose uptake, and gene expression in 3T3-L1 cells. *Endocrinology* **136,** 1474–1481 (1995).
18. Braissant, O., Foufelle, F., Scotto, C., Dauca, M. & Wahli, W. Differential expression of peroxisome proliferator-activated receptors (PPARs): tissue distribution of PPAR-alpha, -beta, and -gamma in the adult rat. *Endocrinology* **137,** 354–366 (1996).
19. Greene, M. E. *et al.* Isolation of the human peroxisome proliferator activated receptor gamma cDNA: expression in hematopoietic cells and chromosomal mapping. *Gene Express.* **4,** 281–299 (1995).
20. Devchand, P. R. *et al.* The PPARalpha-leukotriene B4 pathway to inflammation control. *Nature* **384,** 39–43 (1996).
21. Yu, K. *et al.* Differential activation of peroxisome proliferator-activated receptors by eicosanoids. *J. Biol. Chem.* **270,** 23975–23983 (1995).
22. Meade, E. A., Smith, W. L. & DeWitt, D. L. Differential inhibition of prostaglandin endoperoxide synthase (cyclooxygenase) isozymes by aspirin and other non-steroidal anti-inflammatory drugs. *J. Biol. Chem.* **268,** 6610–6614 (1993).
23. Lau, C. S., Morley, K. D. & Belch, J. J. Effects of fish oil supplementation on non-steroidal anti-inflammatory drug requirement in patients with mild rheumatoid arthritis—a double-blind placebo controlled study. *Br. J. Rheumatol.* **32,** 982–989 (1993).
24. Feldmann, M., Brennan, F. M. & Maini, R. N. Role of cytokines in rheumatoid arthritis. *Annu. Rev. Immunol.* **14,** 397–440 (1996).
25. Brennan, F. M. & Feldman, M. Cytokines in autoimmunity. *Curr. Opin. Immunol.* **8,** 872–877 (1996).
26. Moreland, L. W. Treatment of rheumatoid arthritis with a recombinant human tumor necrosis factor receptor (p75)-Fc fusion protein. *N. Engl. J. Med.* **337,** 141–147 (1997).
27. McEvoy, G. K. (ed) *AHFS 97 Drug Information* (American Society of Health-Systems Pharmacists, Bethesda, MD, 1997).
28. Firestein, G. S. & Zvaifler, N. J. Anticytokine therapy in rheumatoid arthritis. *N. Engl. J. Med.* **337,** 195–197 (1997).

Acknowledgements. We thank T. Gulick for advice, guidance, time and key reagents. This work was supported by a grant from Amgen, Inc., and awards from the NIH. A.T. is a fellow of the Cancer Research Institute.

Correspondence and requests for materials should be addressed to B.S. (e-mail: seed@molbio.mgh.harvard.edu).

G-protein-coupled receptor of Kaposi's sarcoma-associated herpesvirus is a viral oncogene and angiogenesis activator

Carlos Bais*†, Bianca Santomasso*†, Omar Coso‡‖, Leandros Arvanitakis§‖, Elizabeth Geras Raaka¶, J. Silvio Gutkind‡, Adam S. Asch†, Ethel Cesarman§, Marvin C. Gerhengorn¶ & Enrique A. Mesri*†

** Laboratory of Viral Oncogenesis, † Division of Hematology–Oncology, and ¶ Division of Molecular Medicine, Department of Medicine, and § Department of Pathology, Cornell University Medical College, New York, New York 10021, USA*
‡ Molecular Signaling Unit, Laboratory of Cellular Development and Oncology, NIDR, NIH, Bethesda, Maryland 20892, USA

The Kaposi's sarcoma-associated herpesvirus (KSHV/HHV8) is a γ-2 herpesvirus[1–5] that is implicated in the pathogenesis of Kaposi's sarcoma[1,5] and of primary effusion B-cell lymphomas (PELs)[6]. KSHV infects malignant and progenitor cells of Kaposi's sarcoma[7] and PEL[2,6,8], it encodes putative oncogenes[4,5,9] and genes that may cause Kaposi's sarcoma pathogenesis by stimulating angiogenesis[4,5,9,10]. The G-protein-coupled receptor encoded by an open reading frame (ORF 74) of KSHV[9] is expressed in Kaposi's sarcoma lesions and in PEL[9,11] and stimulates signalling pathways linked to cell proliferation[12] in a constitutive (agonist-independent) way[12]. Here we show that signalling by this KSHV G-protein-coupled receptor leads to cell transformation and tumorigenicity, and induces a switch to an angiogenic phenotype[13] mediated by vascular endothelial growth factor[14], an angiogenesis[13,14] and Kaposi's-spindle-cell growth factor[15–17]. We find that this receptor can activate two protein kinases, JNK/SAPK and p38MAPK, by triggering signalling cascades like those induced by inflammatory cytokines[18] that are angiogenesis activators[19] and mitogens for Kaposi's sarcoma cells[10] and B cells. We conclude that the KSHV G-protein-coupled receptor is a viral oncogene that can exploit cell signalling pathways to induce transformation and angiogenesis in KSHV-mediated oncogenesis.

Persistently activated G-protein-coupled receptors (GPCRs) can transform cells[20] and act as oncogenes in human cancers[21]. To determine whether the constitutively active KSHV-GPCR was oncogenic, we used a focus-formation assay in NIH3T3 cells. Transfection of NIH3T3 cells with the expression vector pCEFL-KSHV-GPCR (pCKSHV-GPCR) led to dose-dependent appearance of foci of transformation three weeks after transfection, whereas cells transfected with pCEFL vector did not form any foci (Table 1). The pCEFL and pCKSHV-GPCR constructs showed similar transfection efficiency but only pCKSHV-GPCR induced foci of transformation; the transforming potency of KSHV-GPCR was comparable to that of the m1 muscarinic receptor (m1 AChR), and agonist-dependent transforming GPCR[20] (Table 1). All pCKSHV-GPCR-transformed cells and all pCKSHV-GPCR transiently or stably transfected cells expressed KSHV-GPCR, as determined by polymerase chain reaction with reverse transcription (RT-PCR) (not shown), and accumulated significantly more inositol phosphate (InsP) second messenger molecules[12] than did pCEFL-transfected cells. Six NIH3T3 cell clones stably expressing KSHV-GPCR constitutively produced 2.8 ± 1.6-fold more InsP than did pCEFL-transfected clones ($P < 0.05$), and two neo-enriched populations of cells expressing KSHV-GPCR produced InsP at rates that were sixfold faster than pCEFL-transfected populations. These results indicate that in all these transfected NIH3T3 cells, the KSHV-GPCR gene was not only expressed but its gene product was biologically active and signalling. To show that cell transformation is a result of KSHV-GPCR signalling, we investigated the effects of GPCR-specific kinases (GRKs), which phosphorylate and inhibit activated GPCRs[22], on their signalling. We found that GRK-5, a GRK that can desensitize KSHV-GPCR signalling[23], gave up to a 60% inhibition of focus formation (Fig. 1), whereas GRK-2, which

Table 1 Cell-transforming and tumorigenic activity of KSHV-GPCR

Plasmid	Neo^r colonies*	Foci of cell transformation†	Tumour forming clones‡
pCEFL	3,500	0	0/3
pCEFL-KSHV-GPCR	2,800	400	3/4
pCMV-m1 AchR§	3,000	680	ND
pCEFL-RasV12‖	2,500	2,000	ND

NIH3T3 cells was transfected with 0.2 or 2 μg of plasmid DNA as described in Methods. ND, not determined.
* Efficiency of transfection was determined by plating the transfected cells in medium containing 750 μg ml^{-1} of G418.
† Foci of transformation were scored after 3 weeks for the GPCRs and after 10 d for RasV12. Formation of foci was dependent on the dose of transfected DNA; focus formation potency was determined by extrapolating the data from 0.2 μg transfected DNA. Results represent the median of three experiments. The morphology of foci obtained with KSHV-GPCR was similar to m1 AchR-induced foci (see Supplementary Information).
‡ Transformed cells from representative foci selected in neomycin, or cells stably transfected with pCEFL, were injected into BALB/c nude mice ($n = 4$). Tumour formation was scored after a month. The three tumorigenic clones produced tumours in all four mice injected. The three pCEFL stably transfected clones did not produce tumours in any of the four mice injected.
§ The m1 AchR (pCMVm1) was used as a positive control for GPCR-induced transformation[20] after transfection cells were cultured in the presence of 100 μM carbachol[20].
‖ RasV12 (pCEFL RasV12) was used as a positive control for agonist-independent focus formation.

‖ Present addresses: Molecular Virology Laboratory, Hellenic Pasteur Institute, Athens GR-115 21, Greece (L.A.); Laboratorio de Fisiologia y Biologia Molecular, Dept de Cs. Biologicas, F.C.E. y N. Universidad de Buenos Aires, Buenos Aires, Argentina (O.C.).

Nature © Macmillan Publishers Ltd 1998

does not affect KSHV-GPCR signalling, did not affect focus formation even at high doses (Fig. 1). This indicates that transformation is a consequence of signalling triggered by KSHV-GPCRs.

Focus-derived transformed cells were selected in neomycin and injected into the flank of nude mice. Three of the four tested KSHV-GPCR-transformed clones caused tumours (Table 1, Fig. 2a); the time taken for a 1.5-cm^3 tumour to form ranged from 10 days to 4 weeks, whereas none of the pCEFL stable transfectants were tumorigenic (Table 1, Fig. 2b). The tumours had the histomorphological features of fibrosarcomas (Fig. 2c) and were formed by plump spindle cells with relatively abundant eosinophilic cytoplasm. Cells were atypical, with vesicular nuclei and prominent nucleoli, and mitotic figures were easily identified. Cells removed from freshly dissected tumours and selected in neomycin expressed KSHV-GPCR and produced large amounts of inositol phosphate (not shown), indicating that a strong KSHV-GPCR activity was associated with the tumorigenic state. These results show that in NIH3T3 cells, KSHV-GPCR is an oncogene that triggers intracellular signalling cascades leading to cell transformation and tumorigenicity.

KSHV-GPCR is most homologous to the human receptor for the angiogenic chemokine interleukin-8 (ref. 24), and we showed previously that KSHV-GPCR signalling stimulates transcription controlled by AP-1-containing promoters[12], such as those controlling the expression of several angiogenic growth factors[25]. KSHV-GPCR could, therefore, induce angiogenesis or evoke angiogenic-like signalling. KSHV-GPCR-transformed cells formed vascularized tumours (Fig. 2b), indicating that either the cells were angiogenic before the mouse injection, or that they went through an angiogenic switch[13] while growing '*in vivo*'. As angiogenicity cannot be correlated with KSHV-GPCR expression in transformed cells because they can undergo further genetic changes that affect angiogenicity, we tested whether KSHV-GPCR induces angiogenicity using transiently or stably transfected NIH3T3 cells. We tested conditioned medium from pCKSHV-GPCR-transfected cells and controls for ability to induce endothelial cell growth and angiogenesis '*in vitro*'. Figure 3a, b shows that in all states post-transfection, and for all stably transfected clones, media conditioned by KSHV-GPCR-expressing cells could stimulate growth of human umbilical vein endothelial cells (HUVECs). In contrast, conditioned medium from cells and clones transfected with pCEFL, like untransfected NIH3T3 cells, could not support endothelial cell growth (Fig. 3a, b). To confirm the angiogenicity *in vitro* of pCKSHV-GPCR-transfected

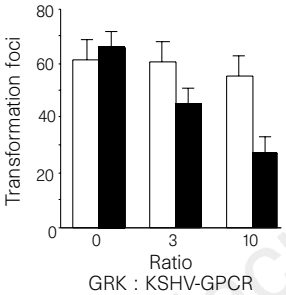

Figure 1 Inhibition of KSHV-GPCR-induced focus formation by GRK-5. Focus-forming activity of KSHV-GPCR in NIH3T3 cells in the presence of GRK-5 and GRK-2. NIH3T3 cells were transfected with 0.2 μg pCKSHV-GPCR alone or with 0.6 μg or 2 μg of GRK-5 (black bars) or GRK-2 (white bars) plasmid. Data represent the mean ± range of duplicate determinations in one representative experiment.

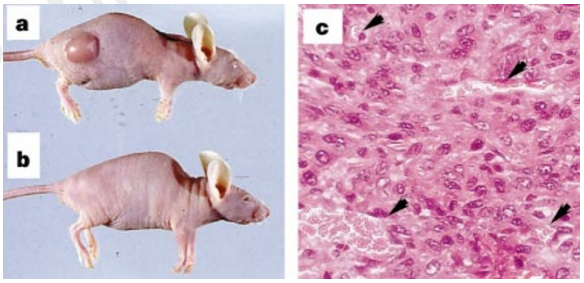

Figure 2 Tumorigenicity of KSHV-GPCR-transformed NIH3T3 cells in nude mice. **a**, **b**, Photographs of mice taken 10 d after injection with cells **a**, from KSHV-GPCR-induced focus of transformation, or **b**, stably transfected with pCEFL vector. **c**, Microscopic appearance of a tumour stained with haematoxylin–eosin (original magnification, ×400). Arrows indicate blood vessels.

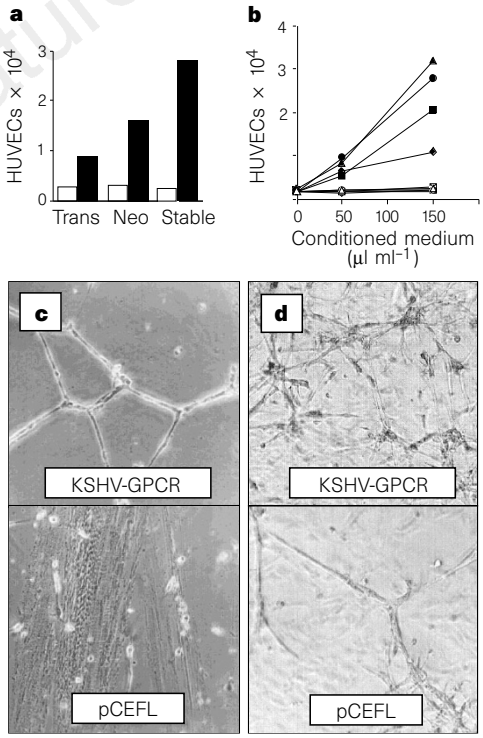

◀ **Figure 3** Angiogenic response *in vitro* induced by NIH3T3 cells transfected with KSHV-GPCR. **a**, **b**, Paracrine stimulation of endothelial cell growth (HUVECs). **a**, Mitogenicity to HUVECs of conditioned medium from NIH3T3 cells transfected with pCKSHV-GPCR (black bars) or pCEFL (white bars). Trans, transient transfection; Neo, cell populations enriched in transfectants by mass selection in neomycin; Stable, stable transfectants. **b**, Mitogenicity to HUVECs of conditioned medium from KSHV-GPCR (filled symbols) or pCEFL (open symbols) stably transfected clones and non-transfected NIH3T3 cells (open triangles). Experiments show the mean of duplicate determinations in one representative experiment; all duplicates deviated from their means by less than 10%. **c**, Microtubule formation *in vitro* induced by conditioned medium from transfected cells. Photographs show the appearance of the matrigel surface 24 h after seeding the HUVECs in the presence of different conditioned media (phase contrast; original magnification, ×100). Note the formation of interconnected microtubules in the endothelial cells incubated with KSHV-GPCR-conditioned medium. **d**, Microtubule formation *in vitro* in matrigel by coincubation of HUVECs with transfected cells. Transfected cells were incubated with HUVECs seeded in the top of the matrigel; note the increase in microtubule formation and the invasion of the tridimensional matrix by HUVECs incubated with KSHV-GPCR-transfected cells (bottom of the plate/background cells). Photographs show the appearance of the matrigel surface 48 h after incubation (phase contrast; original magnification, ×100).

Nature © Macmillan Publishers Ltd 1998

Nature © Macmillan Publishers Ltd 1998

clones, we tested their conditioned media in a microtubule-formation assay[26] and in a co-culture matrigel assay[27]. Figure 3c shows that conditioned medium from pCKSHV-GPCR-transfected cells induced formation of endothelial cell microtubules in matrigel, whereas control medium did not. HUVECs seeded over a matrigel layer covering the cells transfected with pCKSHV-GPCR (Fig. 3d) invaded the matrigel to form a network of interconnecting microtubules[27], whereas pCEFL-transfected cells induced background microtubule formation on top of the matrigel layer (Fig. 3d). These results indicate that expression of KSHV-GPCR is sufficient to produce an imbalance between secreted angiogenic inducers and inhibitors which leads to a switch to an angiogenic phenotype[13]. Vascular endothelial growth factor is a major angiogenic inducer[13,14] and KS-spindle-cell growth factor[15–17] that can be transcriptionally regulated by the AP-1-responsive promoter in the VEGF gene[25]. Figure 4a shows that conditioned than did medium from cells transfected with pCKSHV-GPCR contained from two (transient transfection) to six (neomycin-enriched and stable transfectants) times more VEGF than did medium from pCEFL-transfected cells (Fig. 4a) or non-transfected NIH3T3 cells (not shown). VEGF levels strongly correlated with the stimulation of endothelial cell growth ($r = 0.92$), suggesting that VEGF might mediate this mitogenic response. To test whether angiogenic responses *in vitro* are mediated by VEGF, we used an anti-mouse-VEGF antibody, which specifically blocks VEGF activity. As shown in Fig. 4d, anti-VEGF antibody inhibited responses induced by conditioned medium from pCKSHV-GPCR-transfected cells both in the endothelial cell growth assay and in the microtubule formation assay (Fig. 4b–d). These results show that VEGF, a well characterized mediator of physiological and pathological angiogenesis, and a KS-spindle-cell growth factor, also controls the KSHV-GPCR-induced angiogenic switch.

Our results indicate that this KSHV gene subverts cell signalling pathways leading to oncogenesis and angiogenicity. The three principal kinase cascades that mediate signalling between membrane receptors and the nucleus in mammalian cells are the ERK-2/MAPK kinase cascade induced by mitogen activation of tyrosine-kinase receptors and Ras, and the JNK/SAPK and p38MAPK pathways induced by inflammatory cytokines and stress[18]. To investigate the signalling pathways activated by KSHV-GPCR, we expressed epitope-tagged MAPK/ERK-2, JNK/SAPK or p38MAPK together with KSHV-GPCR in HEK 293T cells and found that KSHV-GPCR could activate JNK/SAPK and p38MAPK but not ERK-2/MAPK (Fig. 5); these data indicate that constitutive signalling by KSHV-GPCR can recruit protein kinase pathways characteristic of activation by inflammatory cytokines[18]. These results are consistent with the idea that KSHV-GPCR signalling in KSHV-infected cells can mimic signalling by agonists that cause proliferation of Kaposi's sarcoma and B cells, and that are Kaposi's-spindle-cell angiogenesis activators[19].

We have presented three lines of evidence indicating that KSHV-GPCR can participate in KSHV-mediated oncogenesis. We found that KSHV-GPCR, which is expressed in KSHV-associated malignancies[9,11], can transform cells and induce tumorigenicity. It is still not known whether KSHV-mediated transformation occurs as with Epstein-Barr virus (EBV/HHV-4), as a consequence of genetic modifications in immortalized latently infected proliferating cells[28], or as an event occurring during productive infection as a result of an abortive lytic cycle. KSHV-GPCR is an early lytic gene

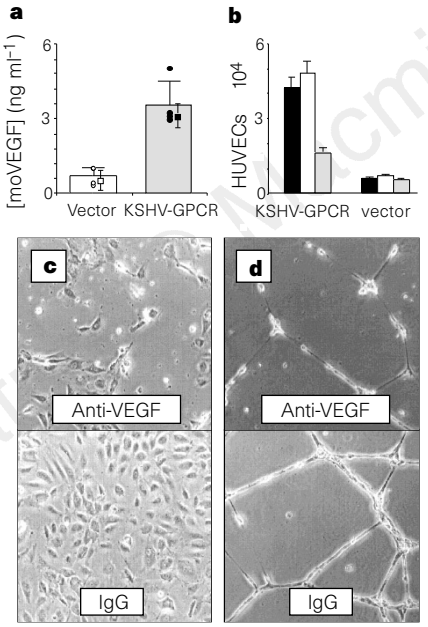

Figure 4 The angiogenic response induced by KSHV-GPCR is mediated by VEGF. **a**, Levels of VEGF measured by ELISA. Results are the mean of duplicate determinations in one representative experiment; duplicates deviated from their means by less than 5%. Cells transfected with pCEFL are represented by white circles; cells transfected with KSHV-GPCR by black circles. **b**, **c**, Anti-VEGF antibody inhibits endothelial cell mitogenicity of media conditioned by KSHV-GPCR-transfected NIH3T3 cells. **b**, Conditioned media were incubated with no addition (black bars), preimmune goat total IgG (white bars) or anti-mouse VEGF antibody (grey bars). Data represent the mean ± range of duplicate determinations in one representative experiment. **c**, Appearance of endothelial cells after incubation with conditioned medium two days after plating (phase contrast; original magnification, ×100). **d**, Anti-VEGF antibody inhibits *in vitro* microtubule-formation activity of media conditioned by KSHV-GPCR-transfected NIH3T3 cells. Before assay, the conditioned media were incubated with the antibodies indicated. Photographs show the appearance of the microtubules after 24 h incubation (phase contrast; original magnification, ×100).

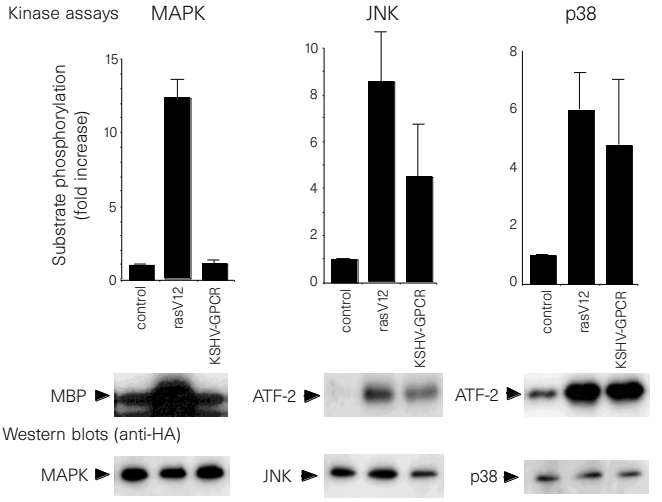

Figure 5 KSHV-GPCR can activate members of the MAPK superfamily. HEK 293T cells were transfected with pcDNA3-HA-ERK2, pcDNA3-HA-JNK or pCEFL-HA-p38 (1 μg per plate), together with pcDNA3 vector (control) or with pCKSHV-GPCR as indicated (2 μg per plate in each case). As positive controls, cells were co-transfected with an activated mutant of *ras* (pCEFL RasV12) or stimulated with anisomycin (10 μg ml^{-1}) for ERK2 (MAPK) or JNK and p38, respectively. Kinase reactions were performed on anti-HA immunoprecipitates from the corresponding lysates. A fraction of the total lysates was used for western blotting analysis. Autoradiograms correspond to representative experiments. ^{32}P-labelled products, as well as specific bands detected by the anti-HA antibody, are indicated by arrows. Data represent the mean ± s.e.m. of three independent experiments and are expressed as fold increase with respect to vector-transfected cells (control).

Nature © Macmillan Publishers Ltd 1998

that shows basal expression in latently infected populations and is expressed in *de novo* infections (R. Nador and O. Flore, personal communications), indicating that it could participate in both types of oncogenesis. We have shown that KSHV-GPCR expression is sufficient to induce a switch to an angiogenic phenotype by secretion of VEGF, an angiogenesis growth factor[13,14] and Kaposi's sarcoma cell mitogen. KSHV-GPCR is expressed in Kaposi's sarcoma lesions and induction of the angiogenic phenotype and VEGF secretion by KSHV-GPCR can therefore participate in autocrine or paracrine stimulation of the KS angiogenic and proliferative response. Finally, we have shown that KSHV-GPCR can activate JNK/SAPK and p38 MAPK kinases, indicating that this viral protein has the molecular specificity to trigger both signalling cascades activated by inflammatory cytokines[18] that induce angiogenicity and upregulate VEGF in Kaposi's spindle cells[17,19] and induce a Kaposi's sarcoma phenotype in endothelial cells. Our results suggest that 'signalling mimicry' by KSHV-GPCR in KSHV-infected cells could activate an inflammatory-cytokine-like signalling pathway leading to angiogenesis and point to possible mechanisms for chemokine-induced angiogenesis[24]. To our knowledge, this is the first demonstration that a KSHV gene is capable of inducing both transformation and an angiogenic phenotype in mammalian cells, strongly supporting the concept that KSHV infection plays a direct role in Kaposi's sarcoma pathogenesis and lymphomagenesis. □

Methods

Cell transfection and focus formation assays. To express KSHV-GPCR in NIH3T3 cells (Swiss mouse), a KSHV-GPCR DNA fragment obtained from pKSHVGPCR[12] (pcDNA3-KSHVGPCR, CMV promoter) was subcloned into the pCEFL plasmid (mouse EF 12 promoter), which also codes for neomycin resistance, to obtain pCEFL-KSHV-GPCR (pCKSHV-GPCR). All transfections were carried out by the calcium phosphate method[20]. Focus formation was assayed as described[20]. For neomycin enrichment, cells were incubated in DMEM with 10% calf serum (Bio-Whittaker) plus 750 $\mu g\,ml^{-1}$ of G418 (Geneticin, Gibco-BRL). To obtain clonal stable transfectants, the selected neomycin plates were split in order to obtain isolated colonies. pCKSHV-GPCR and pCEFL stable transfectants were maintained in 750 $\mu g\,ml^{-1}$ G418 and always passaged before confluence.

Tumorigenicity studies. Transformed cells from foci were isolated by trypsinization within a cloning cylinder, and grown in DMEM with 10% calf serum, 750 $\mu g\,ml^{-1}$ G418. For injection, cells were trypsinized, resuspended in PBS and injected in the right flank of 8–10-week-old female BALB/c nu/nu mice (3×10^5 cells per 200 μl PBS per animal).

Inositol phosphate accumulation. InsP accumulation was determined as described[12]. InsP accumulation during 90 min was calculated as the difference between InsP levels in cells incubated with or without LiCl. InsP levels were normalized as a percentage of the total ^3H radioactivity in inositol phosphates plus lipids.

Endothelial cell growth assay. Fresh HUVECs (passage 4 to 6) were grown in gelatin-coated plates with M199 medium 20% FBS, 2 $ng\,ml^{-1}$ bFGF (GIBCO-BRL). The HUVECs were seeded in gelatin-free 24-well plates (10^4 cells per plate) and the mitogenicity assay was carried out as described[29]. Conditioned medium was obtained from preconfluent cultures by incubation with neomycin-free medium (with or without calf serum) during 48 h.

Microtubule formation in matrigel *in vitro*. Wells of a 24-multiwell plate were coated with 100 μl per well of liquid extracellular matrix extract (Sigma) or Matrigel (Collaborative Biomed) and incubated for 30 min at 37 °C. HUVEC cells (10^4) in medium with 10% calf serum were added per well and conditioned medium was added once cells were attached. Plates were observed after 24 h. For co-culture experiment, matrigel was added on top of transfected cell and microtubule formation was allowed to proceed for 2–3 d.

VEGF ELISA. VEGF in the conditioned medium was measured using a mouse-VEGF Quantikine kit (R&D), following the manufacturer's recommended procedures. For calibration, we used mVEGF standards provided with the kit.

Anti-VEGF antibody inhibition of angiogenic activity *in vitro*. Conditioned media were incubated with 0.2 $\mu g\,ml^{-1}$ of anti-mouse-VEGF polyclonal antibody (total goat IgG; R&D) or with preimmune total goat IgG (R&D) for 1 h room temperature. The preincubated conditioned media were used in HUVEC assays and matrigel microtubule formation assays.

Kinase assays. Phosphorylating activities of transfected, epitope-tagged MAPK, JNK and p38 MAPK were determined as described[30]. Cleared cell lysates were immunoprecipitated with anti-HA monoclonal antibody and an *in vitro* kinase assay was performed using myelin basic protein (MBP) or GST–ATF2 as substrates for MAPK or JNK and p38, respectively.

Western blots. Western blot analysis using anti-HA epitope antibody was done using a fraction of the total lysates as described[30].

Received 11 July; accepted 7 October 1997.

1. Chang, Y. *et al.* Identification of herpesvirus-like DNA sequences in AIDS-associated Kaposis's sarcoma. *Science* **266,** 1865–1869 (1994).
2. Mesri, E. A. *et al.* Human herpesvirus-8/Kaposi's sarcoma-associated herpesvirus is a new transmissible virus that infects B-cells. *J. Exp. Med.* **183,** 2385–2390 (1996).
3. Renne, R. *et al.* Lytic growth of Kaposi's sarcoma associated herpesvirus (HHV-8) in culture. *Nature Med.* **2,** 342–346 (1996).
4. Russo, J. L. *et al.* Nucelotide sequence of the Kaposi's sarcoma associated herpesvirus (HHV8). *Proc. Natl Acad. Sci. USA* **93,** 14862–14867 (1997).
5. Boshoff, C. & Weiss, R. A. Kaposis sarcoma-associated herpesvirus. *Curr. Opin. Infect. Dis.* **10,** 26–31 (1997).
6. Cesarman, E., Chang, Y., Moore, P. S., Said, J. W. & Knowles, D. M. Kaposi's sarcoma-associated herpesvirus-like DNA sequences are present in AIDS-related body cavity B-cell lymphomas. *N. Engl. J. Med.* **332,** 1186–1191 (1995).
7. Boshoff, C. *et al.* Kaposi's sarcoma-associated herpesvirus infects endothelial and spindle cells. *Nature Med.* **1,** 1274–1278 (1995).
8. Arvanitakis, L. *et al.* Establishment and characterization of a body cavity-based lymphoma cell line (BC-3) harboring Kapos's Sarcoma-associated herpesvirus (KSHV/HHV-8) in the absence of EBV. *Blood* **86,** 2708–2714 (1996).
9. Cesarman, E. *et al.* Kaposis sarcoma-associated herpesvirus contains G protein-coupled receptor and cyclin D homologs which are expressed in Kaposis sarcoma and malignant lymphoma. *J. Virol.* **70,** 8218–8223 (1996).
10. Ensoli, B., Barillari, G. & Gallo, R. C. Cytokines and growth factors in the pathogenesis of AIDS-associated Kaposi's Sarcoma. *Immunol. Rev.* **127,** 147–155 (1992).
11. Guo, H. G. *et al.* Characterization of a chemokine receptor-related gene in human herpesvirus 8 and its expression in Kaposi's sarcoma. *Virology* **228,** 371–378 (1997).
12. Arvanitakis, L., Geras Raaka, E., Varma, A., Gershengorn, M. & Cesarman, E. Human herpesvirus KSHV encodes a constitutively active G-protein coupled receptor linked to cell proliferation. *Nature* **385,** 347–350 (1997).
13. Hanahan, D. & Folkman, J. Patterns and emerging mechanisms of the angiogenic switch during tumorigenesis. *Cell* **86,** 356–364 (1996).
14. Ferrara, N. Vascular endothelial growth factor. *Eur. J. Cancer* **14,** 2413–2422 (1996).
15. Masood, R. *et al.* Vascular endothelial growth factor/vascular permeability factor is an autocrine growth factor in AIDS-Kaposi's sarcoma. *Proc. Natl Acad. Sci. USA* **94,** 979–984 (1997).
16. Nakamura, S., Murakamimori, K., Rao, N., Weich, H. A. & Rajeev, B. Vascular endothelial growth factor is a potent angiogenic factor in aids-associated kaposis-sarcoma-derived spindle cells. *J. Immunol.* **158,** 4992–5001 (1997).
17. Cornali, E. *et al.* Vascular endothelial growth factor regulates angiogenesis and vascular permeability in kaposis sarcoma. *Am. J. Pathol.* **149,** 1851–1869 (1996).
18. Kyriakis, J. M. & Avruch, J. Sounding the alarm—Protein kinase cascades activated by stress and inflammation. *J. Biol. Chem.* **271,** 24313–24316 (1996).
19. Samaniego, F., Markham, P. D., Gallo, R. C. & Ensoli, B. Inflammatory cytokines induce AIDS-Kaposi's sarcoma-derived spindle cells to produce and release basic fibroblast growth factor and enhance Kaposi's sarcoma-like lesion formation in nude mice. *J. Immunol.* **154,** 3582–3592 (1994).
20. Gutkind, S., Novotny, E. A., Brann, M. R. & Robbins, K. C. Muscarinic acetylcholine receptors as agonist dependent oncogenes. *Proc. Natl Acad. Sci. USA* **88,** 4703–4707 (1991).
21. Van Sande, J. *et al.* Genetic basis of endocrine disease: Somatic and germline mutations of the TSH receptor gene in thyroid diseases. *J. Clin. Endocr. Metab.* **80,** 2577–2585 (1995).
22. Premont, R. T., Inglese, J. & Lefkowitz, R. J. Protein kinases that phosphorylate activated G-protein coupled receptors. *FASEB J.* **9,** 175–182 (1995).
23. Geras Raaka, E. *et al.* Inhibitionof constitutive signalling of Kaposi's sarcoma associated herpesvirus G protein coupled receptor by protein kinases in mammalian cells in culture. *J. Exp. Med.* (submitted).
24. Koch, A. E. *et al.* Interleukin-8 as a macrophage mediator of angiogenesis. *Science* **258,** 1798–1801 (1992).
25. Kolch, W., Martiny-Baron, G., Kieser, A. & Marme, D. Regulation of the expression of the VEGF/VPS and its receptors: role in rumor angiogenesis. *Breast Cancer Res. Treat.* **36,** 139–155 (1995).
26. Goto, F., Goto, K., Weindel, K. & Folkman, J. Synergistic effects of vascular endothelial growth factor and basic fibroblast growth factor on the proliferation and cord formation of bovine capillary endothelial cells within collagen gels. *Lab. Invest.* **69,** 508–517 (1993).
27. Montesano, R., Pepper, M. S. & Orci, L. Paracrine induction of angiogenesis *in vitro* by Swiss 3T3 fibroblasts. *J. Cell Sci.* **105,** 1013–1024 (1993).
28. Rickinson, A. B. & Kieff, E. in *Fields Virology* 3rd edn (eds Fields, B. N., Knipe, D. M. & Howley, P. M.) 2397–2446 (Lippincott-Raven, Philadelphia, 1996).
29. Mesri, E. A., Federoff, H. J. & Brownlee, M. Expression of vascular endothelial growth factor from a defective herpes simplex virus type 1 amplicon vector induces angiogenesis in mice. *Circ. Res.* **76,** 161–167 (1995).
30. Coso, O. A. *et al.* The small GTP-binding proteins Rac1 and Cdc42 regulate the activity of the JNK/SAPK signaling pathway. *Cell* **81,** 1137–1146 (1995).

Supplementary information is available on *Nature*'s World-Wide Web site (http://www.nature.com) or as paper copy from Mary Sheehan at the London editorial office of *Nature*.

Acknowledgements. We thank G. Lam for HUVECs, R. Nador and O. Flore for sharing data and for comments, and A. Chadburn for help with histopathological characterization. Plasmids encoding GRK-2 and GRK-5 were a gift from R. J. Lefkowitz. This work was supported by NIH grants from NIAID to E.A.M., from NCI to E.C., and from NIDDK to M.C.G.

Correspondence and requests for materials should be addressed to E.A.M. (e-mail: eamesri@mail.med.cornell. edu).

Nature © Macmillan Publishers Ltd 1998

fractions were loaded on a reverse-phase column and eluted using a linear gradient of 2–80% acetonitrile. DC-CK1 protein concentration was estimated by densitometric scanning of a coomassie blue-stained gel containing lysozyme as a standard. RANTES, MIP-1α and IL-8 were obtained from R&D Systems. T-cell migration was measured using 48-well chemotaxis chambers (Neuroprobe) as described[19]. In brief, chemokines in RPMI-1640 were added to the lower chamber and were separated from 10^5 cells in RPMI-1640 with 10% FCS by either a 8-μm or a 5 μm PVP-free polycarbonate membrane (Poretics, Livermore). After incubation for 1 h, the membrane was removed and the upper side washed with PBS, scraped to remove residual cells and washed again. After methanol fixation and staining, the number of fully migrated cells was counted microscopically in 5 high-power fields (× 400) per well. Pertussis toxin (100 ng ml^{-1}) (Calbiochem) was used for 2 h. Each experiment was performed in duplicate, and experiments with DC-CK1, RANTES, MIP-1α and IL-8 were performed in parallel in the same assay to make a direct comparison of their activities possible.

***In situ* hybridization.** Cryosections (8 μm) of tonsils and lymph nodes were fixed in 4% paraformaldehyde and pretreated with 2 μg ml^{-1} pepsin in 0.2 M HCl for 10 min and 0.1 M triethanol amine/0.25 acetic acid anhydride for 10 min. Sections were hybridized overnight with either a sense or an antisense DIG-labelled DC-CK1 RNA probe consisting of the 3′ non-coding region generated by *in vitro* transcription (Boehringer Mannheim). Before incubation with anti-DIG-alkaline phosphatase monoclonal antibody the sections were treated with 40 U ml^{-1} RNAse I (Promega) to ensure specificity. After incubation for 2–3 h with nitroblue tetrazolium/5-bromo-4-chloro-3-indolyl phosphate (Boehringer Mannheim) the sections were stained with methylene green and embedded in Kaiser's. Immunostaining was performed as described[20].

Received 30 December 1996; accepted 24 April 1997.

1. Steinman, R. M. The dendritic cell system and its role in immunogenicity. *Annu. Rev. Immunol.* **9,** 271–296 (1991).
2. Marland, G., Bakker, A. B. H., Adema, G. J. & Figdor, C. G. Dendritic cells in immune response induction. *Stem Cells* **14,** 501–507 (1997).
3. Oppenheimer, J. J., Zachariae, C. O. C., Mukaida, N. & Matsushima, K. Properties of the novel proinflammatory supergene intercine cytokine family. *Annu. Rev. Immunol.* **9,** 617–648 (1991).
4. Schall, T. in *The Cytokine Handbook* (ed. Thompson, A.) 418–460 (Academic, New York, 1994).
5. Sallusto, F. & Lanzavecchia, A. Efficient presentation of soluble antigen by cultured human dendritic cells is maintained by granulocyte/macrophage colony-stimulating factor plus interleukin 4 and downregulated by tumor necrosis factor alpha. *J. Exp. Med.* **179,** 1109–1118 (1994).
6. Romani, N. *et al.* Proliferating dendritic cell progenitors in human blood. *J. Exp. Med.* **180,** 83–93 (1994).
7. Bakker, A. B. H. *et al.* Generation of anti-melanoma CTL from healthy donors after presentation of melanoma associated antigen derived epitopes by dendritic cells in vitro. *Cancer Res.* **55,** 5330–5334 (1995).
8. Baumhueter, S. *et al.* Binding of L-selectin to the Vascular sialomucin CD34. *Science* **262,** 436–438 (1993).
9. Grouard, G., Durand, I., Filgueira, L., Banchereau, J. & Liu, Y.-J. Dendritic cells capable of stimulating T cells in germinal centers. *Nature* **384,** 364–367 (1996).
10. Schall, T. J., Bacon, K., Toy, K. J. & Goeddel, D. V. Selective attraction of monocytes and T lymphocytes of the memory phenotype by cytokine RANTES. *Nature* **347,** 669–672 (1991).
11. Schall, T. J., Bacon, K., Camp, R. D. R., Kaspari, J. W. & Goeddel, D. V. Human Mip-1α and Mip-1B chemokines attract distinct Populations of lymphocytes. *J. Exp. Med.* **177,** 1821–1825 (1993).
12. Ross, J. S., Mistry, K., Bacon, K. B. & Camp, R. D. Characterisation of the *in vitro* responsiveness of lymphocyte subsets to locomotor stimuli by immunocytochemical methods. *J. Immunol. Meth.* **140,** 219–225 (1991).
13. Katz, A., Wu, D. & Simon, M. I. Subunits βγ of heterotrimeric G protein activate γ2 isoform of phospholipase C. *Nature* **360,** 686–689 (1992).
14. Peters, J. H., Gieseler, R., Thiele, B. & Steinbach, F. Dendritic cells: from ontogenic orphans to myelomonocytic descendants. *Immunol. Today* **17,** 273–278 (1996).
15. Cocchi, F. *et al.* Identification of RANTES, Mip-1α and Mip-1β as the major HIV-suppressive factors produced by CD8+ T cells. *Science* **270,** 1811–1815 (1995).
16. Premack, B. A. & Schall, T. J. Chemokine receptors: Gateways to inflammation and infection. *Nature Med.* **11,** 1174–1178 (1996).
17. Figdor, C. G., Bont, W. S., Touw, I., Roosnek, E. E. & de Vries, J. E. Isolation of functionally different human monocytes by counterflow centrifugation elutriation. *Blood* **60,** 46–53 (1982).
18. Groningen, van J. J., Bloemers, H. P. & Swart, G. W. Identification of melanoma inhibitory activity and human melanoma cell lines with different metastatic capacity by messenger RNA differential display. *Cancer Res.* **15,** 6237–6243 (1995).
19. Bacon, K. B., Camp, R. D., Cunningham, F. M. & Woollard, P. M. Contrating in vitro lymphocyte chemotactic activity of the hydroxyl enantiomers of 12-hydroxy-5,8,10,14-eicosatetraenoic acid. *Br. J. Pharmacol.* **95,** 966–972 (1988).
20. Mattijssen, V. *et al.* Clinical and immunopathological results of a phase II study of perilymphatically injected recombinant IL-2 in locally far advanced head and neck squamous cell carcinoma. *J. Immunother.* **10,** 63–68 (1991).

Acknowledgements. We thank S. Zurawski, D. Gorman, F. Vega, R. Kastelein, M. Bell, K. Franz-Bacon, D. Figueroa, M. Koningswieser, R. Huijbens, C. Maass and L. Schalkwijk for assistance, and G. Zurawski, D. Ruiter and P. de Mulder for support. The DNAX Research Institute is supported by Schering Ploung Corporation.

Correspondence and requests for materials should be addressed to G.J.A. (e-mail: g.adema@dent.kun.nl).

A GPI-linked protein that interacts with Ret to form a candidate neurturin receptor

Robert D. Klein*¶, Daniel Sherman*, Wei-Hsien Ho*, Donna Stone*, Gregory L. Bennett†, Barbara Moffat‡, Richard Vandlen‡, Laura Simmons§, Qimin Gu§, Jo-Anne Hongo‖, Brigitte Devaux‖, Kris Poulsen*, Mark Armanini*, Chika Nozaki¶, Naoya Asai¶, Audrey Goddard§, Heidi Phillips*, Chris E. Henderson#, Masahide Takahashi¶ & Arnon Rosenthal*

*Departments of * Neuroscience, † BioAnalytical Technology, ‡ Protein Biochemistry, § Molecular Biology and ‖ Antibody Technology, Genentech, Inc., 460 Point San Bruno Boulevard, South San Francisco, California 94080, USA*
¶ Department of Pathology, Nagoya University School of Medicine, 65 Tsurumai-cho, Showa-ku, Nagoya 466, Japan
 # INSERM U.382, Developmental Biology Institute of Marseille, 13288 Marseille 09, France
§ Present address: Deltagen, Inc., 1031 Bing Street, San Carlos, California 94070, USA

Glial-cell-line-derived neurotrophic factor (GDNF) and neurturin (NTN) are two structurally related, potent survival factors for sympathetic, sensory and central nervous system neurons[1–6]. GDNF mediates its actions through a multicomponent receptor system composed of a ligand-binding glycosyl-phosphatidylinositol (GPI)-linked protein (designated GDNFR-α) and the transmembrane protein tyrosine kinase Ret[7–12]. In contrast, the mechanism by which the NTN signal is transmitted is not well understood. Here we describe the identification and tissue distribution of a GPI-linked protein (designated NTNR-α) that is structurally related to GDNFR-α. We further demonstrate that NTNR-α binds NTN (K_d~10 pM) but not GDNF with high affinity; that GDNFR-α binds to GDNF but not NTN with high affinity; and that cellular responses to NTN require the presence of NTNR-α. Finally, we show that NTN, in the presence of NTNR-α, induces tyrosine-phosphorylation of Ret, and that NTN, NTNR-α and Ret form a physical complex on the cell surface. These findings identify Ret and NTNR-α as signalling and ligand-binding components, respectively, of a receptor for NTN and define a novel family of receptors for neurotrophic and differentiation factors composed of a shared transmembrane protein tyrosine kinase and a ligand-specific GPI-linked protein.

In searching for a neurturin receptor, we examined sequences deposited in public databases for similarity to the GDNF receptor α component (GDNFR-α)[9,10]. Eight partial human cDNAs (Genbank accession numbers R02249, H12981, W73681, W73633, H05619, R02135, T03342 and HSC1KA111) were identified and found to encode parts of a single protein of 464 amino acids which we designated neurturin receptor α (NTNR-α). The human proteins hNTNR-α and hGDNFR-α display an overall 48% similarity, and the positions of their cysteine residues are conserved (Fig. 1). Both hNTNR-α and hGDNFR-α seem to be extracellular proteins that are attached to the outer cell membrane by means of a glycosyl-phosphatidyl inositol (GPI) modification. hNTNR-α has an amino-terminal signal peptide for secretion, three glycosylation sites, and a stretch of 17 carboxy-terminal hydrophobic amino acids preceded by a group of three small amino acids (Gly, Ser, Asn) defining a cleavage/binding site for GPI linkage (Fig. 1). Subsequently, a rat NTNR-α (rNTNR-α) was isolated and shown to be 94% identical to its human homologue (Fig. 1).

To examine whether NTNR-α could be a receptor for a neurotrophic factor such as NTN, the tissue distribution of NTNR-α mRNA was examined by *in situ* hybridization and compared with

Nature © Macmillan Publishers Ltd 1997

that of GDNFR-α (Fig. 2 and data not shown). In the embryonic rat nervous system, mRNA for NTNR-α was found in the ventral midbrain where dopaminergic neurons are located, in parts of the ventral spinal cord where motor neurons are present and in the dorsal root ganglia (DRG) where sensory neurons reside. In addition, high levels of NTNR-α transcripts were found in developing sympathetic ganglia and peripheral nerves. Low levels of NTNR-α mRNA were detected in non-neuronal tissues, such as smooth and striated muscle of the embryonic gut, oesophagus, diaphragm and limb bud, which express high levels of GDNFR-α transcripts. In the adult rat brain, NTNR-α mRNA was detected in the substantia nigra, cortex, olfactory bulb and the dorsal horn of the spinal cord. Although NTNR-α mRNA and GDNFR-α mRNA were often coexpressed, the two transcripts occasionally displayed distinct tissue distribution. For instance, in the limb, GDNFR-α is expressed mainly in muscle cells but also around the brachial plexus, which innervates the muscle, whereas NTNR-α is found mainly in the brachial plexus. Similarly, in the embryonic bladder, NTNR-α is expressed in the muscle layer, whereas GDNFR-α is expressed in the underlying epithelia. Finally, in the gut, NTNR-α is expressed in the mucosal epithelium as well as in smooth muscle whereas GDNFR-α is expressed only in smooth muscle (Fig. 2). This pattern of expression is consistent with the hypothesis that NTNR-α mediates signals both inside and outside the nervous system, and suggests overlapping, yet distinct, biological roles for NTNR-α and GDNFR-α.

To determine whether NTNR-α could function as a receptor for NTN, binding experiments were performed. Equilibrium binding of human or mouse ^{125}I-NTN to recombinant soluble human (data not shown) or rat NTNR-α protein demonstrated that NTN binds specifically and reversibly to NTNR-α, and that the two proteins associate with an approximate K_d of 10 pM (Fig. 3). In contrast, neither human nor mouse NTN (at 1 nM) were able to displace ^{125}I-rGDNF from rGDNFR-α, and no binding of human or mouse ^{125}I-NTN to rGDNFR-α was detected. Taken together, these data are consistent with the idea that NTN interacts at high affinity solely with NTNR-α (Fig. 3). Although no high-affinity interaction between NTN and GDNFR-α was detected, we did observe, using higher concentrations of unlabelled NTN (10 nM), displacement of ^{125}I-rGDNF from GDNFR-α, suggesting that there is a low-affinity interaction between NTN and GDNFR-α ($K_d > 1$ nM) (data not shown).

To examine further whether NTNR-α is a specific receptor for NTN, competition binding experiments were performed using ^{125}I-rGDNF. Displaceable high-affinity binding of ^{125}I-rGDNF to recombinant soluble rGDNFR-α was readily observed ($K_d = 3$ pM) (Fig. 3), but no binding of ^{125}I-rGDNF (iodinated either on primary amino groups by using the Bolton-Hunter method, or on tyrosines by using the lactoperoxidase method) could be detected to either hNTNR-α or rNTNR-α. Similarly, no significant displacement of ^{125}I-labelled mouse NTN (^{125}I-mNTN) from NTNR-α was detected in the presence of unlabelled rGDNF (up to 1 nM). Thus GDNF seems to bind with high affinity to GDNFR-α but not to NTNR-α. As before, displacement of ^{125}I-mNTN from NTNR-α was observed when a high concentration (10 nM) of unlabelled GDNF was used, suggesting a low-affinity interaction between GDNF and NTNR-α ($K_d > 1$ nM) (data not shown). The specific high-affinity interactions between GDNF and GDNFR-α, and NTN and NTNR-α, were confirmed using competition binding to intact cells that express individual receptors (data not shown). Consistent with the prediction that NTNR-α is anchored to the cell surface by a GPI linkage, the binding of ^{125}I-NTN to cells expressing NTNR-α was significantly reduced by treatment with phosphoinositide-specific phospholipase C (PIPLC), an enzyme that specifically cleaves GPI linkages[13] (Fig. 4a). Taken together, these findings support the idea that NTNR-α is a high-affinity, GPI-linked binding protein for NTN, and that GDNFR-α is a specific high-affinity binding protein for GDNF.

Consistent with the idea that NTNR-α participates in the response to NTN, we found that NTN can prevent the death of two populations of neurons that express NTNR-α: primary embryonic dopaminergic neurons (data not shown), and motor neurons (Fig. 4b). Moreover, in agreement with the finding that NTN and GDNF use distinct receptors, we detected differences in the efficacy (but not in the potency) of the two factors. Whereas GDNF at saturating concentrations promoted the survival of 100% of BDNF-responsive motor neurons, NTN prevented the death of only 50% of these cells (Fig. 4b).

To confirm that NTNR-α is a required mediator of the NTN signal, embryonic motor neurons were treated with PIPLC, and their survival in the presence of NTN or BDNF was monitored in culture. The capacity of saturating concentrations of NTN to support the survival of embryonic rat motor neurons was completely abolished by PIPLC treatment, whereas no decrease in the

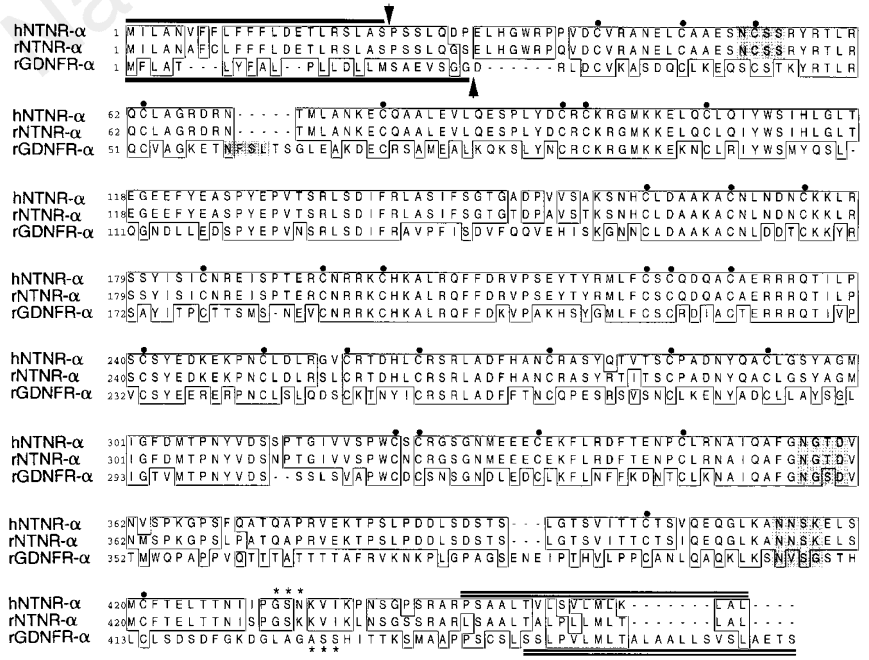

Figure 1 Primary structure of NTNR-α, and their homology to rat GDNFR-α. Signal peptides are indicated by solid lines, putative signal peptide cleavage sites are marked with arrows, potential glycosylation sites are shaded, the hydrophobic domains of the GPI attachment sites are doubly underlined, the small amino-acid residues that constitute the cleavage/attachment site for GPI-linked proteins are marked with asterisks, and the consensus cysteine residues are indicated by filled circles.

Nature © Macmillan Publishers Ltd 1997

Nature © Macmillan Publishers Ltd 1997

response of motor neurons to brain-derived neurotrophic factor (BDNF) was caused by PIPLC. Moreover, when NTN was added to PIPLC-treated motor neurons in combination with soluble NTNR-α, the response to NTN (Fig. 4c), but not to GDNF (data not shown), was restored. Thus NTNR-α is a necessary and specific component of the NTN signalling cascade and has the properties expected of the ligand-binding subunit of a functional NTN receptor.

NTNR-α, like GDNFR-α, lacks a cytoplasmic domain and is anchored to the outer surface of the cell by GPI. Thus, transmission of the NTN signal to the interior of the cell must involve additional proteins. As the tyrosine-kinase receptor Ret, which by itself does not bind GDNF[9,10] or NTN (data not shown), was found to be a signalling component of the GDNF receptor, we examined the possibility that it would also transduce the NTN signal following binding of NTN to NTNR-α. The human neuroblastoma TGW-I-nu cell line, which expresses endogenous c-*ret*[14,15], was exposed to NTN for 5 min, and the level of Ret tyrosine phosphorylation was determined. NTN induced phosphorylation of Ret (Fig. 4d), as well as two isoforms of the cytoplasmic kinase ERK (MAP kinase) (Fig. 4e) in this cell line. Furthermore, consistent with the idea that NTNR-α is a necessary mediator of the response to NTN, only residual tyrosine phosphorylation of Ret in response to NTN was observed in PIPLC-treated TGW-I-nu cells (Fig. 4d). The amount of tyrosine-phosphorylated Ret protein was greatly increased in PIPLC-treated TGW-I-nu cells when NTN was added together with a soluble NTNR-α (Fig. 4d).

As these findings suggested that Ret participates in the transmission of the NTN signal, we investigated whether it is part of a putative NTN receptor complex. TGW-I-nu cells were exposed to NTN and then lysed with a mild detergent. Protein complexes were immunoprecipitated with a polyclonal antibody to Ret and then analysed on a western blot using a polyclonal antibody to NTN. Consistent with the idea that NTN and Ret interact physically on the cell surface, NTN was readily co-immunoprecipitated by Ret antibodies (Fig. 4f). To confirm that NTNR-α is also present in the NTN–Ret protein complex, human embryonic kidney 293 cells were transiently transfected with c-*ret* alone, with an epitope-tagged NTNR-α alone, or with a combination of expression vectors for c-*ret* and an epitope-tagged NTNR-α, and were exposed to NTN before being lysed with a mild detergent[16]. Protein complexes were then immunoprecipitated with polyclonal antibody to Ret and analysed on a western blot using a monoclonal antibody to the epitope-tagged NTNR-α. No protein complex could be detected in cells that were transfected with Ret alone or with NTNR-α alone, either in the presence or absence of NTN (Fig. 4g, and data not shown). In contrast, in cells that expressed both proteins, residual NTNR-α could be co-immunoprecipitated by Ret antibodies in the absence of NTN. Further, addition of NTN led to a significant increase in the amount of NTNR-α that could be co-immunoprecipitated by the Ret antibodies (Fig. 4g). These findings support the hypothesis that NTN, NTNR-α and Ret form a complex on the cell surface; that Ret and NTNR-α are components of a functional NTN receptor; and that NTNR-α is an important intermediary in the interaction between NTN and Ret.

Taken together, our results define a candidate receptor for NTN and demonstrate the existence of a family of multicomponent receptors composed of a shared signalling subunit, the transmembrane tyrosine kinase receptor Ret, and receptor-specific ligand-binding subunits that are GPI-linked (Fig. 5). The findings are consistent with the observation that Ret-deficient mice display more severe deficits in the superior cervical ganglion sympathetic

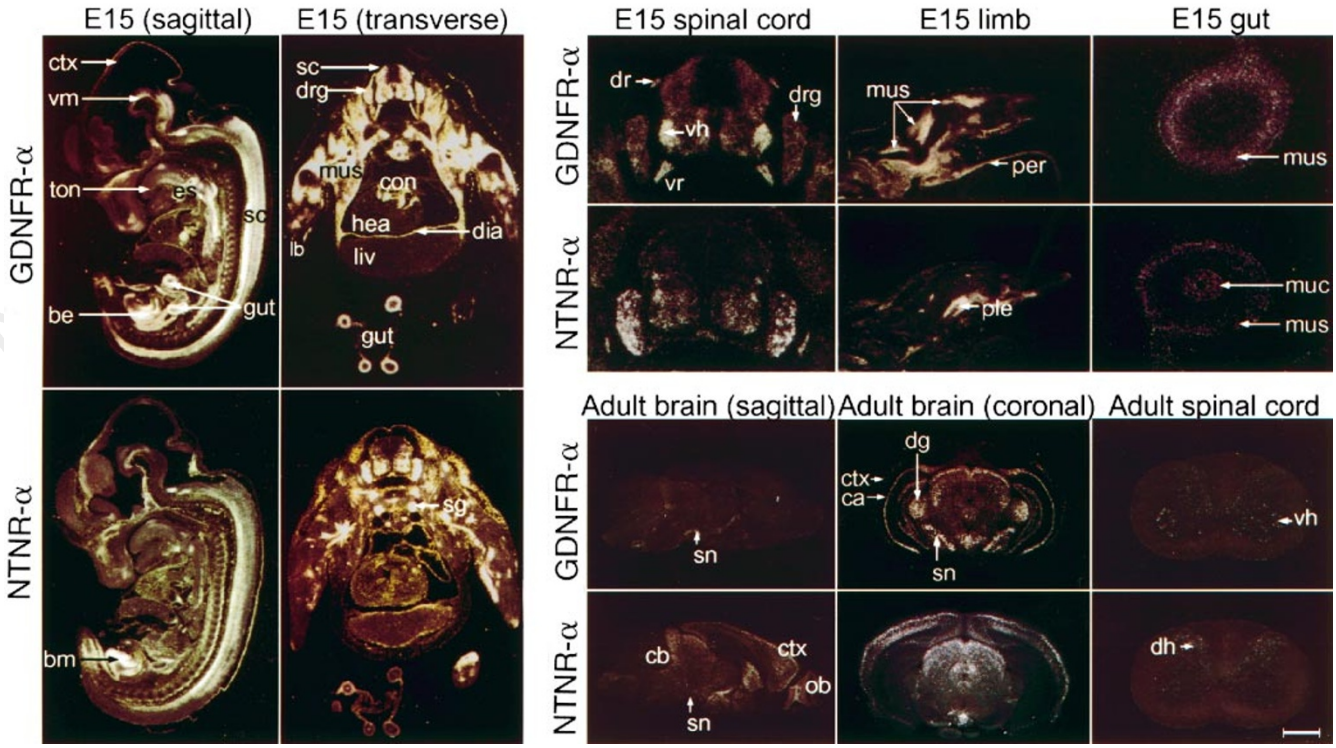

Figure 2 Tissue distribution of mRNA for NTNR-α and GDNFR-α. Abbreviations: vm, ventral midbrain; es, oesophagus; ctx, cortex; sc, spinal cord; ton, tongue; be, bladder epithelium; sg, sympathetic ganglia; bm, bladder muscles; dia, diaphragm; mus, muscle; con, cardiac conductive system; sn, substantia nigra; dg, dentaqte gyrus; ob, olfactory bulb, cb, cerebellum; ca, cornus ammonis; dr, dorsal root; drg, dorsal root ganglia; vr, ventral root; vh, ventral horn; muc, mucosal epithelial; pte, brachial plexus nerves; liv, liver; hea, heart. Scale bar, 1.1 mm in E15 sagittal section; 800 μm in E15 transverse section; 240 μm in E15 spinal cord; 590 μm in E15 limb; 93 μm in E15 gut; 3.6 mm in adult brain (sagittal); 2.4 mm in adult brain (coronal); 900 μm in adult spinal cord. The E15 transverse and spinal cord sections were exposed for different times.

Nature © Macmillan Publishers Ltd 1997

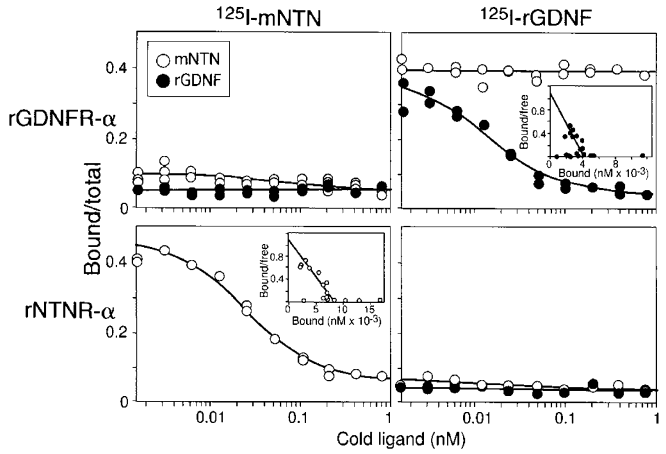

Figure 3 Binding of iodinated NTN and GDNF to NTNR-α and GDNFR-α. Binding of ^{125}I mouse NTN (^{125}I-mNTN) (5 pM) or ^{125}I rat GDNF (^{125}I-rGDNF) (5 pM) to rat NTNR-α (rNTNR-α) or rat GDNFR-α (rGDNFR-α). Human NTNR-α displayed a similar binding specificity to rat NTNR-α (data not shown). As depicted by the Scatchard analysis (insets), GDNF binds GDNFR-α with an approximate K_d value of 3 pM (similar K_d values were reported in a cell-based assay[10]), and NTN binds NTNR-α with an approximate K_d value of 10 pM.

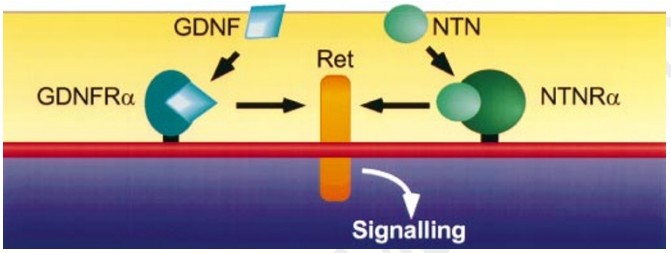

Figure 5 A schematic representation of activation of Ret by NTN or GDNF. NTN and GDNF each bind to a unique GPI-linked ligand-binding protein. This ligand-binding protein complex can bind to and activate a shared transmembrane tyrosine kinase receptor, Ret.

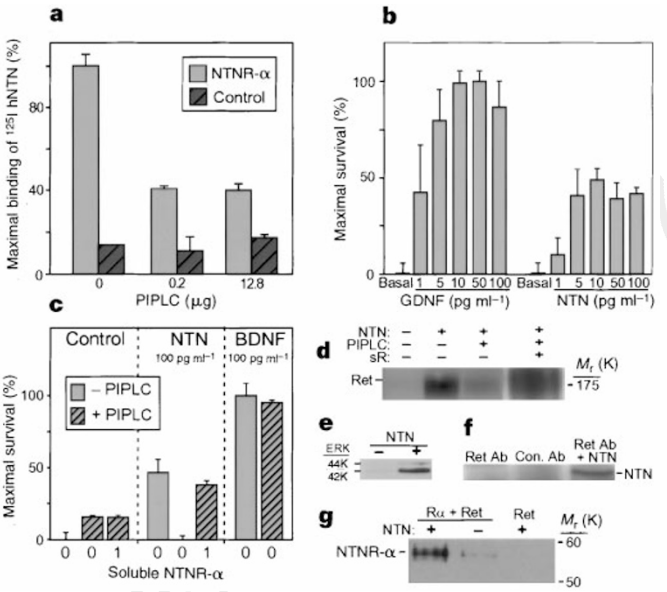

Figure 4 Interaction between NTN, NTNR-α and Ret. **a**, Binding of ^{125}I-NTN to cells expressing NTNR-α was reduced by 60% after treatment with PIPLC. **b**, Survival response of embryonic rat spinal motor neurons to GDNF or NTN, expressed as a percentage of the maximal survival in the presence of GDNF. In agreement with its receptor distribution, NTN is a potent survival factor for spinal motor neurons. **c**, Survival response of embryonic, rat spinal motor neurons to NTN or BDNF in the presence of PIPLC and soluble NTNR-α. PIPLC treatment completely abolished the survival response to NTN without changing the response to BDNF. Soluble NTNR-α restored the response of PIPLC-treated motor neurons to NTN. **d**, NTN induces tyrosine phosphorylation of Ret in TGW-I-nu cells. Phosphorylation was significantly reduced in the presence of PIPLC and is restored in the presence of soluble NTNR-α (SR). **e**, NTN induces phosphorylation of ERK in TGW-I-nu cells. **f**, NTN and Ret form a complex in TGW-I-nu cells. **g**, Recombinant NTNR-α and Ret form a protein complex in 293 cells. The amount of this protein complex is significantly increased in the presence of NTN. Ret, cells transfected with Ret alone. Rα + Ret, cells transfected with Ret and NTNR-α.

neurons[17,18] than GDNF-deficient mice[19–21] and suggest that the distinct biological activities of the GDNF and NTN may be determined by the different tissue distributions of their respective ligand-binding receptor components, rather than by their ability to activate different signalling systems.

Our findings provide a biological rationale for the evolution of what appeared to be a needlessly complex way to activate a tyrosine kinase[22]. With the discovery that Ret is shared by GDNF and NTN, it is now apparent that changing the ligand-binding molecule allows recruitment of the same signalling system by multiple growth factors. Similar 'cost-effective' strategies to make use of a single transmembrane signalling system by multiple growth factors appear to be used by cytokines[16,23], members of the transforming growth factor protein family[24], and bacterial endotoxins[25,26].

The discovery of this receptor system further defines a new model of signal transduction and highlights the diverse strategies that are used to transmit extracellular signals in the vertebrate nervous system. □

Methods

NTNR-α cloning and expression constructs. The partial cDNA sequence encoded by the expressed sequence tag (EST) cDNA clones was extended using 5′ and 3′ Marathon RACE reactions (Clontech) on human spleen mRNA, using conditions supplied by the manufacturer. Additional cDNA clones for NTNR-α were identified by screening a human fetal brain cDNA library (Stratagene) and a rat brain cDNA library (Clontech) using standard protocols. For mammalian protein expression, the complete open reading frame (ORF) was amplified using PCR and cloned into a CMV-based expression vector. The NTNR-α–IgG expression construct was made by cloning the first 432 amino acids of the receptor (which lacks a GPI linkage site) in front of the human Fc (IgG2a) sequence. For co-precipitation experiments, an epitope tag was inserted between the signal peptide and the mature coding sequence of NTNR-α. Soluble NTNR-α was produced as a C-terminal His-tagged protein in HEK 293 cells, purified by Ni-NTA chromatography[27], and tested for NTN binding.

***In situ* hybridization.** Rat embryos at embryonic day 15.5 (E15.5) were immersion-fixed overnight at 4 °C in 4% paraformaldehyde, then cryoprotected overnight in 15% sucrose. Adult rat brains and spinal cords were frozen fresh. All tissues were sectioned at 16 μm, and processed for *in situ* hybridization using ^{33}P-UTP labelled RNA probes[3]. Sense and antisense probes were derived for the N-terminal regions of NTNR-α or GDNFR-α using T7 polymerase.

Equilibrium binding analysis. For receptor-binding experiments, conditioned media from 293 cells transiently transfected with the NTNR-α–IgG or GDNFR-α–IgG constructs were incubated with approximately 5 pM ^{125}I-hNTN, ^{125}I-mNTN or ^{125}I-rGDNF, along with the appropriate cold ligand at concentrations between 0.8 nM and 1.56 pM (2-fold dilutions) in PBS containing 2 mg ml^{-1} BSA (Sigma) and 0.05% Brij 96 (Fluka) for 4 h at room temperature (in the absence of cold ligands, 15–25% of the receptors were occupied). Protein A Sepharose CL-4B beads (~50 μl; Pharmacia) were added to each reaction and the receptor–ligand complex was precipitated after

Nature © Macmillan Publishers Ltd 1997

incubation for 1 h at room temperature. After washing with PBS containing 0.2 mg ml^{-1} BSA, specific counts were measured. The IGOR program was used to determine K_d. Cell-based equilibrium binding analysis[9] was used to confirm the specificity of GDNFR-α and NTNR-α for GDNF and NTN, respectively. Each binding experiment was repeated at least 4 times. For PIPLC analysis, 293 cells transiently transfected with either the full-length NTNR-α expression construct or an irrelevant plasmid were incubated with ~20,000 c.p.m. ^{125}I-hNTN in the presence of the indicated amounts of PIPLC for 90 min at room temperature. The cells were washed with ice-cold PBS containing 0.2 mg ml^{-1} BSA, and cell-associated ^{125}I was measured.

Survival assays. E14 rat motor neurons were purified, plated and grown in duplicate wells in L15 medium with the N2 supplement and 2% horse serum[28]. After 3 days in culture, only 30–40% of the motor neurons initially present survived in basal medium, whereas at saturating concentrations of GDNF or BDNF nearly all motor neurons remained alive. The increase in the number of surviving neurons in the presence of saturating concentrations of GDNF compared to basal medium was taken as 100% (maximal) survival; percentage of maximal survival under the indicated conditions is shown in Fig. 3b. PIPLC (2 μg ml^{-1}) was added to the indicated samples 2 h before, as well as 12 h and 24 h after, addition of the indicated growth factors.

Tyrosine phosphorylation. To assay for tyrosine phosphorylation, cells were incubated for 1 h at 37 °C with or without PIPLC and then exposed to NTN with or without soluble NTNR-α (10 μg ml^{-1}) for 5–10 min at 37 °C. Cells were then removed from the plates with 2 mM EDTA in PBS and lysed with ice-cold buffer (comprising, in mM 10 sodium phosphate (pH 7.0), 100 NaCl, 1% NP40, 5 EDTA, 100 sodium vanadate, 2 mM PMSF, and 0.2 units of aprotinin) and used for immunoprecipitation with antiserum raised against the 19 amino-acid C terminus of Ret, following by binding to protein A–Sepharose. The immunoprecipitated proteins were released by boiling in SDS sample buffer, separated on an 8% SDS-polyacrylamide gel, transferred to a nitrocellulose membrane, and reacted with anti-phosphotyrosine antibody (Upstate Biotechnology). Detection was with an ECL western blotting detection system (Amersham Life Science).

Co-immunoprecipitation. To examine the formation of protein complexes, TGW-I-nu cell were exposed to 500 ng ml^{-1} of NTN. Protein complexes were immunoprecipitated with Ret antibodies, transferred onto a nitrocellulose filter, and analysed with polyclonal antibody against NTN. Alternatively, HEK 293 cells were transiently transfected with expression vectors for Ret, an epitope-tagged NTNR-α, or a combination of an epitope-tagged NTNR-α and Ret. Cells were stimulated with NTN as indicated and lysed with brij 96 detergent (Fluka)[16]. Putative immune complexes were immunoprecipitated with a polyclonal antibody against Ret, transferred onto a nitrocellulose filter, and analysed with a monoclonal antibody against the epitope-tagged NTNR-α.

Received 7 March; accepted 1 May 1997.

1. Lin, L. H., Doherty, D. H., Lile, J. D., Bektesh, S. & Collins, F. GDNF: A glial cell line-derived neurotrophic factor for midbrain dopaminergic neurons. *Science* **260,** 1130–1132 (1993).
2. Kotzbauer, P. T. *et al.* Neurturin, a relative of glial-cell-line-derived neurotrophic factor. *Nature* **384,** 467–470 (1996).
3. Henderson, C. E. *et al.* GDNF: A potent survival factor for motoneurons present in peripheral nerve and muscle. *Science* **266,** 1062–1064 (1994).
4. Buj-Bell, A., Buchman, V. L., Horton, A., Rosenthal, A. & Davies, A. M. GDNF is an age-specific survival factor for sensory and autonomic neurons. *Neuron* **15,** 821–828 (1995).
5. Arenas, E., Trupp, M., Akerud, P. & Ibáñez, C. F. GDNF prevents degeneration and promotes the phenotype of brain noradrenergic neurons in vivo. *Neuron* **15,** 1465–1473 (1995).
6. Trupp, M. *et al.* Peripheral expression and biological activities of GDNF, a new neurotrophic factor for avian and mammalian peripheral neurons. *J. Cell Biol.* **130,** 137–148 (1995).
7. Takahashi, M., Ritz, J. & Cooper, G. M. Activation of a novel human transforming gene, *ret*, by DNA rearrangement. *Cell* **42,** 581–588 (1985).
8. Takahashi, M. & Cooper, G. M. *ret* Transforming gene encodes a fusion protein homologous to tyrosine kinases. *Mol. Cell. Biol.* **7,** 1378–1385 (1987).
9. Treanor, J. J. S. *et al.* Characterization of a multicomponent receptor for GDNF. *Nature* **382,** 80–83 (1996).
10. Jing, S. *et al.* GDNF-induced activation of the ret protein tyrosine kinase is mediated by GDNFR-α, a novel receptor for GDNF. *Cell* **85,** 1113–1124 (1996).
11. Trupp, M. *et al.* Functional receptor for GDNF encoded by the c-*ret* proto-oncogene. *Nature* **381,** 785–789 (1996).
12. Durbec, P. *et al.* GDNF signalling through the Ret receptor tyrosine kinase. *Nature* **381,** 789–793 (1996).
13. Koke, J. A., Yang, M., Henner, D. J., Volwerk, J. J. & Griffith, O. H. High-level expression in *Escherichia coli* and rapid purification of phosphatidylinositol-specific phospholipase C from *Bacillus cereus* and *Bacillus thuringiensis*. *Protein Expr. Purif.* **2,** 51–58 (1991).
14. Ikeda, I. *et al.* Specific expression of the *ret* proto-oncogene in human neuroblastoma cell lines. *Oncogene* **5,** 1291–1296 (1990).
15. Takahashi, M., Buma, Y. & Taniguchi, M. Identification of the *ret* proto-oncogene products in neuroblastoma and leukemia cells. *Oncogene* **6,** 297–301 (1991).
16. Davis, S. *et al.* Released form of CNTF receptor α component as a soluble mediator of CNTF responses. *Science* **259,** 1736–1739 (1993).
17. Schuchardt, A., D'Agati, V., Larsson-Blomberg, L., Costantini, F. & Pachnis, V. Defects in the kidney and enteric nervous system of mice lacking the tyrosine kinase receptor Ret. *Nature* **367,** 380–383 (1996).
18. Durbec, P. L., Larsson-Blomberg, L. B., Schuchardt, A., Costantini, F. & Pachnis, V. *Development* **122,** 349–358 (1996).
19. Pichel, J. G. *et al.* Defects in enteric innervation and kidney development in mice lacking GDNF. *Nature* **382,** 73–76 (1996).
20. Sánchez, M. P. *et al.* Renal agenesis and the absence of enteric neurons in mice lacking GDNF. *Nature* **382,** 70–73 (1996).
21. Moore, M. W. *et al.* Renal and neuronal abnormalities in mice lacking GDNF. *Nature* **382,** 76–79 (1996).
22. Lindsay, R. M. & Yancopoulos, G. D. GDNF in a bind with known orphan: Accessory implicated in new twist. *Neuron* **17,** 571–574 (1996).
23. Ip, N. Y. *et al.* CNTF and LIF act on neuronal cells via shared signaling pathways that involve the IL-6 signal transducing receptor component gp130. *Cell* **69,** 1121–1132 (1992).
24. Wrana, J. L., Attisano, L., Wieser, R., Ventura, F. & Massague, J. Mechanism of activation of the TGF-β receptor. *Nature* **370,** 341–347 (1994).
25. Lee, J.-D. *et al.* Glycosyl-phosphatidylinositol-anchored or integral membrane forms of CD14 mediate identical cellular responses to endotoxin. *Proc. Natl Acad. Sci. USA* **90,** 9930–9934 (1993).
26. Pugin, J. *et al.* Lipopolysaccharide (LPS) activation of human endothelial and epithelial cells is mediated by LPS binding protein and soluble CD14. *Proc. Natl Acad. Sci. USA* **90,** 2744–2748 (1993).
27. Hochuli, E., Dobeli, H. & Schacher, A. New metal chelate adsorbent selective for proteins and peptides containing neighboring histidine residues. *J. Chromatogr.* **411,** 177–184 (1987).
28. Henderson, C. E. *et al.* in *Nerve Cell Culture: A Practical Approach* (eds Cohen, J. & Wilkin, G.) 69–81 (Oxford Univ. Press, 1995).

Acknowledgements. We thank J. Milbrandt and E. Johnson (who were supported by NIH grants) for providing unpublished information and reagents; W. Anstine for preparing the figures; E. Berry for help with the manuscript; A. Ryan for help with the *in situ* hybridization analysis; M. Vasser, P. Jhurani and P. Ng for synthetic oligonucleotides; M. Yang for the PIPLC enzyme; and V. Arce for help with motor neuron cultures. This work was supported in part by INSERM, Association Francaise contre les Myopathies (AFM) and Institut pour la Recherche sur la Moelle Epiniere (IRME) to C.E.H., and by grants-in-aid from scientific research from the Ministry of Education, Science and Culture of Japan to M.T.

Correspondence and requests for materials should be addressed to A.R. (e-mail: ar@gene.com).

Neurturin responsiveness requires a GPI-linked receptor and the Ret receptor tyrosine kinase

Anna Buj-Bello*§, Jimi Adu*§, Luzia G. P. Piñón*, Antony Horton*, Jane Thompson*, Arnon Rosenthal†, Miguel Chinchetru‡, Vladimir L. Buchman* & Alun M. Davies*

** School of Biological and Medical Sciences, Bute Medical Buildings, University of St Andrews, St Andrews, Fife KY16 9AT, UK*
† Department of Neuroscience, Genentech, Inc., 460 Point San Bruno Boulevard, South San Francisco, California 94080, USA
‡ Present address: Departmento de Bioquimica y Biologia Molecular, Facultad de Veterinaria, Universidad de León, 24007 León, Spain
§ These authors contributed equally to this work.

Neurturin (NTN)[1] is a recently identified homologue of glial-cell-line-derived neurotrophic factor (GDNF)[2]. Both factors promote the survival of a variety of neurons[1–5], and GDNF is required for the development of the enteric nervous system and kidney[6–8]. GDNF signals through a receptor complex consisting of the receptor tyrosine kinase Ret and a glycosyl-phosphatidylinositol (GPI)-linked receptor termed GDNFR-α[9–13]. Here we report the cloning of a new GPI-linked receptor termed NTNR-α that is homologous with GDNFR-α and is widely expressed in the nervous system and other tissues. By using microinjection to introduce expression plasmids into neurons, we show that coexpression of NTNR-α with Ret confers a survival response to neurturin but not GDNF, and that coexpression of GDNFR-α with Ret confers a survival response to GDNF but not neurturin. Our findings indicate that GDNF and neurturin promote neuronal survival by signalling through similar multicomponent receptors that consist of a common receptor tyrosine kinase and a member of a GPI-linked family of receptors that determines ligand specificity.

Nature © Macmillan Publishers Ltd 1997